PHYSICAL REVIEW D **94,** 094005 (2016)

Quasidistribution amplitude of heavy quarkonia

Yu Jia[1,2,3,*] and Xiaonu Xiong[4,†]

[1] *Institute of High Energy Physics and Theoretical Physics Center for Science Facilities, Chinese Academy of Sciences, Beijing 100049, China*
[2] *School of Physics, University of Chinese Academy of Sciences, Beijing 100049, China*
[3] *Center for High Energy Physics, Peking University, Beijing 100871, China*
[4] *Istituto Nazionale di Fisica Nucleare, Sezione di Pavia, Pavia 27100, Italy*

(Received 25 December 2015; published 4 November 2016)

The recently proposed quasidistributions point out a promising direction for lattice QCD to investigate the light-cone correlators, such as parton distribution functions and distribution amplitudes (DAs), directly in the x space. Owing to its excessive simplicity, heavy quarkonium can serve as an ideal theoretical laboratory to ascertain certain features of quasi-DAs. In the framework of nonrelativistic QCD factorization, we compute the order-α_s correction to both light-cone distribution amplitudes (LCDAs) and quasi-DAs associated with the lowest-lying quarkonia, with the transverse-momentum UV cutoff interpreted as the renormalization scale. We confirm analytically that the quasi-DA of a quarkonium does reduce to the respective LCDA in the infinite-momentum limit. We also observe that, provided that the momentum of a charmonium reaches about 2–3 times its mass, the quasi-DAs already converge to the LCDAs to a decent level. These results might provide some useful guidance for the future lattice study of quasidistributions.

DOI: 10.1103/PhysRevD.94.094005

I. INTRODUCTION

The QCD factorization theorems [1] imply that the parton distribution functions (PDFs) [2] play the central role in accounting for virtually every high-energy collision experiment. In addition to PDFs, there also exist other important types of light-cone correlators, such as generalized parton distributions (GPDs), transverse-momentum-dependent distributions (TMDs), and light-cone distribution amplitudes (LCDAs), all of which probe the internal structure of a hadron in terms of the fundamental quark-gluon degree of freedom.

These light-cone correlators are of a nonperturbative nature and are notoriously difficult to compute from the first principle of QCD. The eminent obstacle for the lattice simulation originates from the fact that they are defined in terms of the bilocal operators with lightlike separation. In the past, lattice simulation has mainly focused on computing their moments [3–6], which are constructed out of the local operators. Unfortunately, it becomes quickly impractical to go beyond the first few moments, since the more derivatives added, the noisier the lattice simulation would become. To date, our comprehensive knowledge about the nucleon PDF is gleaned exclusively through extracting from the experimental data [7–9].

An exciting breakthrough has emerged recently. A lattice calculation scheme directly in x space was proposed by Ji in 2013 [10]. In this approach, the task of computing the original light-cone correlators is transformed into computing a new class of nonlocal matrix elements: the so-called *quasidistributions*. These quasidistributions are defined as equal-time yet spatially nonlocal correlation functions, thus amenable to the lattice simulation. In contrast to the light-cone quantities, the quasidistributions are generally frame-dependent. But in the infinite-momentum frame (IMF), the quasidistributions are expected to exactly recover the original light-cone distributions. Ji has further envisaged that, in analogy with the heavy quark effective theory, the quasidistribution method can be framed in an effective field theory context, dubbed the *large momentum effective field theory* [11]. The large momentum effective field theory was first applied to proton spin structure, which provides a means to extract the nucleon spin contents from the quasidistributions calculated on a lattice [12,13].

The utility of this new approach hinges crucially on the key that the quasidistributions and light-cone distribution share the exactly same infrared (IR) properties. It implies there exists a factorization theorem that connects these two quantities, with perturbatively calculable matching coefficients. Once the lattice has measured the quasidistributions, one can use this factorization formula to reconstruct the desired light-cone quantities.

During the past two years, the one-loop matching factors have been computed for PDFs, GPDs for the nonsinglet quark, as well as pion DAs [14–16]. The quasi-TMD was also studied in Ref. [17]. Very recently, the two-loop renormalization of a quasi-PDF has also been conducted [18]. The factorization theorem for PDFs has recently been

*jiay@ihep.ac.cn
†Present address: Institute for Advanced Simulation, Institut für Kernphysik,and Jülich Center for Hadron Physics, Forschungszentrum Jülich, D-52425 Jülich, Germany.
x.xiong@fz-juelich.de

proved to all orders in α_s [15]. In addition, there recently have emerged some preliminary results from exploratory lattice simulations, extracting the PDFs from quasi-PDFs through the matching procedure outlined above [19–22]. There are also some new improved formalisms of quasi-PDF are explored in Refs. [23,24].

To turn quasidistributions into a fruitful industry, there remain many technical obstacles to overcome. One outstanding challenge is to systematically implement the renormalization of such nonlocal operators on a lattice. Another difficulty stems from the technical limitation that it is too expensive for the current lattice resources to accommodate a fast-moving hadron on the lattice, since it requires exquisitely fine lattice spacing. It is fair to say that there is still a long way to go for the lattice simulation to be able to produce phenomenologically competitive results.

For the lack of a nonperturbative understanding of quasidistributions, it is worth looking at their features from the perspective of phenomenological models. For example, very recently, the nucleon quasi-PDF has been investigated in a diquark model [25], and the authors have examined how fast the nucleon quasi-PDF would approach the PDF with an increasing nucleon momentum.

Needless to say, it is also highly desirable to gain an understanding about the gross features of the quasidistributions from a model-independent angle. This consideration has motivated us to study the DAs of heavy quarkonia, chiefly because they offer a unique, clean platform to scrutinize the quasidistributions. The key reason is that the DA of the quarkonium can be largely understood solely within the perturbation theory.

The widely separated scales ($m \gg mv, \Lambda_{\rm QCD}$) inherent to quarkonium invites an effective-field-theory treatment. In fact, the influential nonrelativistic QCD (NRQCD) factorization approach [26], which fully exploits this scale hierarchy, nowadays has become an indispensable tool to tackle quarkonium-related phenomena.

According to NRQCD factorization, the LCDA of a heavy quarkonium can be factorized as the sum of the product of perturbatively calculable, IR-finite coefficient functions and nonperturbative local NRQCD matrix elements [27–29]. At the lowest order in velocity expansion, up to a normalization factor, the profile of the quarkonium LCDA is fully amenable to the perturbation theory.

In this work, we generalize this knowledge, apply NRQCD factorization further to the quasi-DA of heavy quarkonia, and calculate the respective coefficient functions to the order of α_s. To keep things as simple as possible, we concentrate on the lowest-lying S-wave quarkonia. We have verified that, like the LCDAs of quarkonium, the quasi-DAs at the order of α_s are also IR-finite. We are able to show analytically that the quasi-DA exactly reduces to the LCDA in the infinity-momentum limit. We also observe that, provided that the quarkonium is boosted to carry a momentum about 2–3 times its mass and with the renormalization scale chosen around the charmonium mass, the respective quasi-DAs will converge to the LCDAs to a satisfactory degree.

We hope some of features about the quarkonium quasi-DAs may also apply to other hadrons. Hopefully, this knowledge will provide some useful guidance to the future lattice investigation of similar quasidistributions.

The rest of the paper is organized as follows. In Sec. II, we present the definitions of LCDAs and quasi-DAs for S-wave quarkonia and discuss the precise meaning of NRQCD factorization to these correlators. In Sec. III, we describe the strategy to determine the DAs of quarkonia beyond tree level, outline the key steps of deriving the one-loop corrections, and present the corresponding analytical expressions for the S-wave quarkonia. In Sec. IV, we carry out a numerical comparison between the LCDA and quasi-DA, to study how fast the quasi-DA approaches the LCDA as the quarkonium momentum increases. We also compare the first inverse moments calculated in both the LCDA and quasi-DA. We summarize in Sec. V. The detailed illustrations about how to work out the one-loop calculation are provided in the Appendixes.

II. NRQCD FACTORIZATION OF QUARKONIUM DISTRIBUTION AMPLITUDES

In contrast to light hadrons, heavy quarkonia are arguably among the simplest hadrons: The constituent quark and antiquark are quite heavy, $m \gg \Lambda_{\rm QCD}$, and move rather slowly ($v \ll 1$). These two essential features result in the hierarchical structure of intrinsic energy scales of a quarkonium. The NRQCD factorization approach [26] fully exploits this scale hierarchy and allows one to efficiently separate the relativistic and perturbative contributions from the long-distance and nonperturbative dynamics. For most quarkonium-related phenomena, i.e., quarkonium production and decay processes, this factorization approach has become a standard tool.

It is well known that the fragmentation functions for a parton transitioning into a light hadron are genuinely nonperturbative objects, and the only way to extract them is through experimental measurements [30]. On the contrary, it was realized long ago that the heavy quarkonium fragmentation function can be put in a factorized form [31,32]. Concretely speaking, for a gluon-to-quarkonium fragmentation function, one has

$$D_{g\to H+X}(z,\mu) = \sum_n d_{g\to c\bar{c}[n]}(z)\langle 0|O_H[n]|0\rangle, \qquad (1)$$

where z denotes the momentum fraction, n specifies the color, spin, or orbital quantum number of the $c\bar{c}$ pair, and $O_H[n]$ is the NRQCD four-fermion operator, which characterizes the transition probability from the partonic state $c\bar{c}[n]$ to the quarkonium H plus additional soft hadrons.

The key insight is that coefficient functions $d_{g\to c\bar{c}[n]}(z)$ are perturbatively calculable.

Analogous to the case of the aforementioned fragmentation function, one might naturally envisage that the DA of a quarkonium is also not a fully nonperturbative object, and some sort of short-distance ($\sim 1/m$) effects should be disentangled owing to asymptotic freedom. Indeed, such an analogy has already been pursued some time ago [27,28]. Schematically, one may express the quarkonium DA in the following factorized form:

$$\Phi_H(x,\mu) \sim \sum_n \langle H|\mathcal{O}_{[n]}|0\rangle \phi_{H[n]}(x,\mu), \tag{2}$$

where the color-singlet NRQCD operators $\mathcal{O}_{[n]}$ are organized according to importance in the velocity expansion. Apart from the universal NRQCD matrix elements, the key observation is that $\phi_{H[n]}(x,\mu)$ can now be interpreted as the short-distance coefficients. Actually, for hard exclusive quarkonium production, employing this factorized quarkonium LCDA turns out to have a considerable advantage compared with the conventional NRQCD factorization approach [33,34].

For simplicity, in this work we will concentrate only on the distribution amplitudes of S-wave quarkonia. Moreover, we will be interested in only the lowest order in v expansion. Obviously, there is no any principal difficulty to incorporate the relativistic corrections or even extend to higher orbital quarkonium states.

A. NRQCD factorization of quarkonium LCDA

To be specific, let us assume the quarkonium H to move along the positive z axis, i.e., $P^\mu = (\sqrt{P_z^2+m^2}, \mathbf{0}_\perp, P^z)$ with $P^z > 0$. For a general 4-vector V^μ, it is convenient to introduce the light-cone plus (minus) components $V^\pm = \frac{1}{\sqrt{2}}(V^0 \pm V^z)$.

The leading-twist LCDAs of the pseudoscalar meson P, longitudinally (transversely) polarized vector meson $V^{\parallel,\perp}$, are defined as

$$\begin{aligned}\Phi_P(x,\mu) &= -if_P P^+ \phi_P(x,\mu)\\ &= \int \frac{d\xi^-}{2\pi} e^{-i(x-\frac{1}{2})P^+\xi^-} \left\langle P(P)\middle|\bar{\psi}\left(\frac{\xi^-}{2}\right)\gamma^+\gamma^5 \mathcal{W}\psi\left(-\frac{\xi^-}{2}\right)\middle|0\right\rangle,\end{aligned} \tag{3a}$$

$$\begin{aligned}\Phi_V^\parallel(x,\mu) &= -if_V^\parallel \varepsilon_\parallel^{*+} M_V \phi_V^\parallel(x,\mu)\\ &= \int \frac{d\xi^-}{2\pi} e^{-i(x-\frac{1}{2})P^+\xi^-} \left\langle V(P,\varepsilon_\parallel)\middle|\bar{\psi}\left(\frac{\xi^-}{2}\right)\gamma^+ \mathcal{W}\psi\left(-\frac{\xi^-}{2}\right)\middle|0\right\rangle,\end{aligned} \tag{3b}$$

$$\begin{aligned}\Phi_V^\perp(x,\mu) &= -if_V^\perp P^+ \phi_V^\perp(x,\mu)\\ &= \int \frac{d\xi^-}{2\pi} e^{-i(x-\frac{1}{2})P^+\xi^-} \left\langle V(P,\varepsilon_\perp)\middle|\bar{\psi}\left(\frac{\xi^-}{2}\right)\gamma^+\gamma\cdot\varepsilon_\perp \mathcal{W}\psi\left(-\frac{\xi^-}{2}\right)\middle|0\right\rangle,\end{aligned} \tag{3c}$$

where $\varepsilon_\parallel^\mu$ and $\varepsilon_\perp^\mu$ are the polarization vectors for the longitudinally and transversely polarized vector meson, respectively, and μ signifies the renormalization scale. $\mathcal{W}$ is the gauge link along the light-cone "minus" direction:

$$\mathcal{W} = \mathcal{P}\exp\left[-ig_s \int_{-\frac{\xi^-}{2}}^{\frac{\xi^-}{2}} d\eta^- A^+(\eta^-)\right]. \tag{4}$$

The decay constants f_H are defined as the vacuum-to-quarkonium matrix elements mediated by various local QCD currents:

$$\langle P(P)|\bar{\psi}\gamma^+\gamma^5\psi|0\rangle \equiv -if_P P^+ = \int_0^1 dx \Phi_P(x,\mu), \tag{5a}$$

$$\langle V(P,\varepsilon_\parallel)|\bar{\psi}\gamma^+\psi|0\rangle \equiv -iM_V f_V^\parallel \varepsilon_\parallel^{*+} = \int_0^1 dx \Phi_V^\parallel(x,\mu), \tag{5b}$$

$$\langle V(P,\varepsilon_\perp)|\bar{\psi}\gamma^+\gamma_\perp\psi|0\rangle \equiv -if_V^\perp P^+\varepsilon_\perp^* = \int_0^1 dx \Phi_V^\perp(x,\mu). \tag{5c}$$

The LCDA is clearly subject to the normalization condition:

$$\int_0^1 dx \phi_H(x) = 1 \quad \forall\ H. \tag{6}$$

Thus far, everything is about the standard definition, valid for any pseudoscalar and vector mesons. So what is special about the heavy quarkonium? As has been argued previously, the quarkonium DA defined above still contains a short-distance contribution, which ought to be identified and isolated.

If H is an S-wave quarkonium state, the precise implication of NRQCD factorization of the LCDA is

$$\phi_H(x) = \phi_H^{(0)}(x) + \frac{C_F\alpha_s}{\pi}\phi_H^{(1)}(x) + \ldots, \tag{7a}$$

$$f_H = f_H^{(0)}\left(1+\frac{C_F\alpha_s}{\pi}\mathfrak{f}_H^{(1)}+\ldots\right)+O(v^2), \tag{7b}$$

where $H = P, V_\parallel, V_\perp$. For the DAs of the hidden-flavor quarkonia (the $c\bar{c}$ or $b\bar{b}$ family), charge conjugation symmetry demands that they are symmetric under $x \leftrightarrow 1-x$.

The key message conveyed in (7) is that the $\phi_H(x)$ entailing all the hard "collinear" degrees of freedom (with a typical virtuality of the order of m^2) thus can be computed in the perturbation theory owing to asymptotic freedom. The nonperturbative aspects of quarkonium are encoded in the decay constant f_H. Moreover, as indicated in (7b), one can match the QCD currents to the respective NRQCD currents, by integrating out the hard quantum fluctuation. Consequently, the genuinely nonperturbative binding dynamics is encapsulated in the NRQCD matrix elements $f_H^{(0)}$. For $H = \eta_c, J/\psi$, one has

$$f_{\eta_c}^{(0)} = \frac{1}{\sqrt{m_c}}\langle \eta_c|\psi^\dagger\chi|0\rangle \approx \sqrt{\frac{N_c}{2\pi m_c}}R_{\eta_c}(0), \tag{8a}$$

$$f_{J/\psi}^{\parallel(0)} = f_{J/\psi}^{\perp(0)} = \frac{1}{\sqrt{m_c}}\langle J/\psi(\varepsilon)|\psi^\dagger\sigma\cdot\varepsilon\chi|0\rangle \approx \sqrt{\frac{N_c}{2\pi m_c}}R_{J/\psi}(0), \tag{8b}$$

where ε denotes the polarization 3-vector in the J/ψ rest frame and $N_c = 3$ is the number of colors in QCD. Since NRQCD matrix elements are always defined in the quarkonium rest frame, rotation invariance then implies that $f_{J/\psi}^{\parallel(0)} = f_{J/\psi}^{\perp(0)}$. As implied in the last entity, these NRQCD matrix elements are often approximated by $R_H(0)$, the radial Schrödinger wave function at the origin for the S-wave charmonia, which can be evaluated in the phenomenological quark potential models.

B. NRQCD factorization of quarkonium quasi-DAs

The quasi-DAs are defined as pure spatial correlation functions and, hence, can be directly simulated on the lattice. Analogous to LCDA (3), we define the quasi-DAs of S-wave quarkonia as

$$\begin{aligned}\tilde{\Phi}_{\eta_c}(x,\mu,P^z) &= -i\tilde{f}_{\eta_c}P^z\tilde{\phi}_{\eta_c}(x,\mu)\\ &= \int\frac{dz}{2\pi}e^{i(x-\frac{1}{2})P^z z}\left\langle \eta_c(P)\middle|\bar{\psi}\left(\frac{z}{2}\right)\gamma^z\gamma^5\mathcal{V}\psi\left(-\frac{z}{2}\right)\middle|0\right\rangle,\end{aligned} \tag{9a}$$

$$\begin{aligned}\tilde{\Phi}^{\parallel}_{\eta_c}(x,\mu,P^z) &= -i\tilde{f}^{\parallel}_{J/\psi}\varepsilon_\parallel^{*z}M_{J/\psi}\tilde{\phi}^{\parallel}_{J/\psi}(x,\mu)\\ &= \int\frac{dz}{2\pi}e^{i(x-\frac{1}{2})P^z z}\left\langle J/\psi(P,\varepsilon_\parallel)\middle|\bar{\psi}\left(\frac{z}{2}\right)\gamma^z\mathcal{V}\psi\left(-\frac{z}{2}\right)\middle|0\right\rangle,\end{aligned} \tag{9b}$$

$$\begin{aligned}\tilde{\Phi}^{\perp}_{J/\psi}(x,\mu,P^z) &= -i\tilde{f}^{\perp}_{J/\psi}P^z\phi^{\perp}_{J/\psi}(x,\mu)\\ &= \int\frac{dz}{2\pi}e^{i(x-\frac{1}{2})P^z z}\left\langle J/\psi(P,\varepsilon_\perp)\middle|\bar{\psi}\left(\frac{z}{2}\right)\gamma^z\boldsymbol{\gamma}\cdot\boldsymbol{\varepsilon}^*_\perp\mathcal{V}\psi\left(-\frac{z}{2}\right)\middle|0\right\rangle,\end{aligned} \tag{9c}$$

where the field separation is along the z direction, and the gauge link $\mathcal{V}$ reads

$$\mathcal{V} = \mathcal{P}\exp\left[-ig_s\int_{-\frac{z}{2}}^{\frac{z}{2}}d\eta^z A^z(\eta^z)\right]. \tag{10}$$

The quasidecay constants, dubbed $\tilde{f}_H$, are again defined as the vacuum-to-quarkonium matrix elements mediated by corresponding QCD currents[1]:

$$\langle\eta_c(P)|\bar{\psi}\gamma^z\gamma^5\psi|0\rangle \equiv -i\tilde{f}_P P^z = \int_{-\infty}^{\infty}dx\tilde{\Phi}_P(x,\mu), \tag{11a}$$

$$\langle J/\psi(P,\varepsilon_\parallel)|\bar{\psi}\gamma^z\psi|0\rangle \equiv -iM_{J/\psi}\tilde{f}^{\parallel}_{J/\psi}\varepsilon_\parallel^{*z} = \int_{-\infty}^{\infty}dx\tilde{\Phi}^{\parallel}_{J/\psi}(x,\mu), \tag{11b}$$

$$\langle J/\psi(P,\varepsilon_\perp)|\bar{\psi}\gamma^z\gamma_\perp\psi|0\rangle \equiv -if^{\perp}_{J/\psi}P^z\varepsilon^*_\perp = \int_{-\infty}^{\infty}dx\tilde{\Phi}^{\perp}_{J/\psi}(x,\mu). \tag{11c}$$

The NRQCD factorization is also valid for the quasi-DAs. For the quasi-DAs of S-wave quarkonia, the precise implication of NRQCD factorization is

[1] Lorentz invariance requires $\tilde{f}_H = f_H$. Here we intentionally distinguish these two cases, because one may choose a UV regulator that does not preserve Lorentz symmetry. In the loop integrals, we will impose a UV cutoff in the transverse-momentum components, which does not to violate the boost invariance along the z axis. Therefore, in our case, we indeed have $\tilde{f}_H = f_H$ and will use them interchangeably.

$$\tilde{\phi}_H(x) = \tilde{\phi}_H^{(0)}(x) + \frac{C_F\alpha_s(\mu)}{\pi}\tilde{\phi}_H^{(1)}(x) + \ldots, \tag{12a}$$

$$\tilde{f}_H = f_H^{(0)}\left(1 + \frac{C_F\alpha_s(2m_c)}{\pi}\mathfrak{f}_H^{(1)} + \ldots\right) + O(v^2), \tag{12b}$$

where $H = P, V_\parallel, V_\perp$. The matching of the decay constant is exactly the same as in (7b).

The quasi-DA is subject to the normalization:

$$\int_{-\infty}^{\infty}\tilde{\phi}_H(x) = 1 \quad \forall\ H. \tag{13}$$

Because a quasi-DA no longer emerges from a parton picture, the integrand is no longer bounded within the interval $x \in [0, 1]$.

In contrast to the LCDA, the quasi-DA is generally dependent on the magnitude of P^z. We note that the heavy quark mass in NRQCD factorization corresponds to a large scale, so it cannot be neglected even in the limit $P^z \gg m$.

III. ONE-LOOP EXPRESSIONS OF DISTRIBUTION AMPLITUDES FOR S-WAVE QUARKONIA

In this section, we compute the one-loop corrections to both LCDAs and quasi-DAs for the S-wave quarkonia, to lowest order in v.

A. Strategy of determining the LCDA and quasi-DA for a quarkonium

The $\phi_H(x)$ $[\tilde{\phi}_H(x)]$ is sensitive only to short-distance dynamics. In order to extract it, it is convenient to replace a physical quarkonium state $|H(P)\rangle$ by a fictitious one, i.e., a pair of free heavy quark-antiquark $|c(p_1)\bar{c}(p_2)\rangle$. We then compute the corresponding $\Phi_{c\bar{c}(P)}(x)$ in the perturbation theory:

$$\Phi_{c\bar{c}(P)}(x) = \Phi_{c\bar{c}}^{(0)}(x) + \frac{C_F\alpha_s(\mu)}{\pi}\Phi_{c\bar{c}}^{(1)}(x) + \ldots, \tag{14a}$$

$$\tilde{\Phi}_{c\bar{c}(P)}(x) = \tilde{\Phi}_{c\bar{c}}^{(0)}(x) + \frac{C_F\alpha_s(\mu)}{\pi}\tilde{\Phi}_{c\bar{c}}^{(1)}(x) + \ldots. \tag{14b}$$

The partonic decay constant $f_{c\bar{c}(P)}$ can also be computed order by order in α_s. Following the definitions in (3) and (9), after projecting onto the suitable quantum number, one should be able to solve for $\phi_H(x)$ $[\tilde{\phi}_H(x)]$ iteratively, order by order in α_s.

The c and $\bar{c}$ in the fictitious charmonium state $|c(p_1)\bar{c}(p_2)\rangle$ carry momenta $p_1 = \frac{P}{2} + q$ and $p_2 = \frac{P}{2} - q$, respectively. Since we are interested in only the lowest order in v, it is legitimate to neglect the relative momentum q; from now on, we thereby assume $p_1 = p_2 = \frac{P}{2} \equiv p$.

When going beyond the tree level, rather than utilize the literal matching method, we take a standard shortcut to directly extract the short-distance coefficient (arising from the hard region m^2) in the loop integral [35]: in the beginning, we simply neglect the relative momentum q prior to carrying out the loop integration.[2] Therefore, our calculation is free from the contamination due to the low-energy effects (loop momentum carrying virtuality of the order of mv or smaller, exemplified by the Coulomb singularity). This brings forth great technical simplification. Nevertheless, the general principle of the effective field theory guarantees that the contributions from the low-energy regimes must cancel between the QCD side and the NRQCD side, and we simply trust it holds and forgo this check.

B. Tree-level results

At the lowest order in α_s, it is straightforward to work out the partonic DAs:

$$\begin{aligned}\Phi^{(0)}_{c(p)\bar{c}(p)}(x,\mu) &= \int\frac{d\xi^-}{2\pi}e^{-i(x-\frac{1}{2})P^+\xi^-}\left\langle c(p)\bar{c}(p)\middle|\bar{\psi}\left(\frac{\xi^-}{2}\right)\gamma^+\Gamma\psi\left(-\frac{\xi^-}{2}\right)\middle|0\right\rangle \\ &= \delta\left(x-\frac{1}{2}\right)\frac{1}{P^+}\bar{u}(p)\gamma^+\Gamma v(p),\end{aligned} \tag{15a}$$

$$\begin{aligned}\tilde{\Phi}^{(0)}_{c(p)\bar{c}(p)}(x,\mu,P^z) &= \int\frac{dz}{2\pi}e^{i(x-\frac{1}{2})P^z z}\left\langle c(p)\bar{c}(p)\middle|\bar{\psi}\left(\frac{z}{2}\right)\gamma^z\Gamma\psi\left(-\frac{z}{2}\right)\middle|0\right\rangle \\ &= \delta\left(x-\frac{1}{2}\right)\frac{1}{P^z}\bar{u}(p)\gamma^z\Gamma v(p),\end{aligned} \tag{15b}$$

$$\langle c(p)\bar{c}(p)|\bar{\psi}\not{n}\Gamma\psi|0\rangle = \frac{1}{n\cdot P}\bar{u}(p)\not{n}\Gamma v(p), \tag{15c}$$

[2] For a one-loop computation of the S-wave quarkonium LCDA following the rigorous NRQCD matching ansatz, we refer the interested reader to Ref. [27].

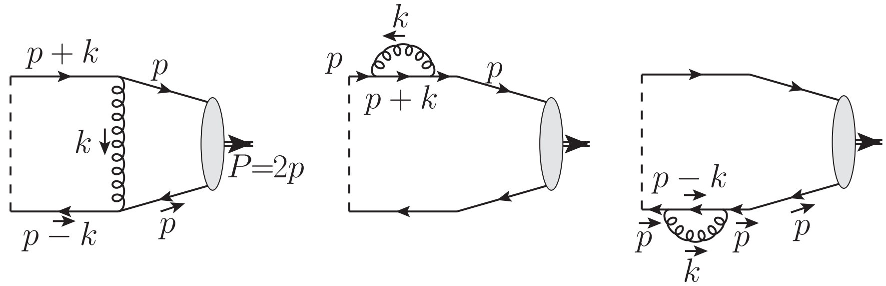

FIG. 1. One-loop diagrams for the S-wave quarkonium (quasi-)DA in the axial gauge.

where we have introduced the reference vector n:

$$n^\mu = \begin{cases} \frac{1}{\sqrt{2}}(1,0,0,-1) & \text{for LCDA,} \\ (0,0,0,-1) & \text{for quasi-DA.} \end{cases} \tag{16}$$

$\Gamma = \gamma^5$, $\mathbf{1}$, $\gamma_\perp^i$ correspond to η_c and the longitudinally and transversely polarized J/ψ meson, respectively.

Since we work with a moving frame of H, it is convenient to adopt the threshold expansion method developed by Braaten and Chen [36], which takes into account the Lorentz transformation between the quarkonium rest frame and the moving frame, making the connection to NRQCD transparent. One then finds

$$\frac{1}{n\cdot P}\bar{u}(p)\not{n}\gamma_5 v(p) = \xi^\dagger\eta|_{c\bar{c}\,\text{rest frame}}, \tag{17a}$$

$$\frac{1}{P^0}\bar{u}(p)\gamma^z v(p) = \xi^\dagger\sigma^z\eta|_{c\bar{c}\,\text{rest frame}}, \tag{17b}$$

$$\frac{1}{P^+}\bar{u}(p)\gamma^+ v(p) = \xi^\dagger\sigma^z\eta|_{c\bar{c}\,\text{rest frame}}, \tag{17c}$$

$$\frac{1}{n\cdot P}\bar{u}(p)\not{n}\gamma_\perp^i v(p) = \xi^\dagger\sigma_\perp^i\eta|_{c\bar{c}\,\text{rest frame}}, \tag{17d}$$

where ξ and η are two-components Pauli spinors. When the $c\bar{c}$ pair is in the ${}^3S_1(\varepsilon)$ state, $\xi^\dagger\boldsymbol{\sigma}\eta \propto \varepsilon$. Everything has the desired structure as dictated in (5); especially, the Lorentz transformation of the longitudinal polarization vector is correctly incorporated. From this knowledge, we can readily determine $f_{c\bar{c}}^0$ for $c\bar{c}({}^1S_0)$ and $c\bar{c}({}^3S_1)$.

Therefore, the tree-level LCDAs and quasi-DAs bear the simple form

$$\phi_H^{(0)}(x) = \tilde{\phi}_H^{(0)}(x) = \delta\left(x-\frac{1}{2}\right), \tag{18}$$

where $H = P$, $V_\parallel$, $V_\perp$. Obviously, it satisfies the normalization condition (5).

Intuitively, this is what is expected from the nonrelativistic limit, when relative momentum is neglected.

C. Outline of one-loop calculation

The DAs of quarkonium will develop a nontrivial profile after implementing a radiative correction. Its shape generally becomes widely spread. This extended profile should not be confused with the LCDAs determined by phenomenological models such as QCD sum rules [37], because it is generated perturbatively and can be computed in a model-independent manner.

We now turn to calculating the order-α_s correction to the LCDA and quasi-DA, that is, to determine $\phi_H^{(1)}$ and $\tilde{\phi}_H^{(1)}$. This can be fulfilled by employing the following relation:

$$\phi_H^{(1)}(x) = \Phi_{c\bar{c}}^{(1)}(x)/\left(\frac{1}{P^+}\bar{u}(p)\gamma^+\Gamma v(p)\right) - \delta\left(x-\frac{1}{2}\right)\mathfrak{f}^{(1)}, \tag{19a}$$

$$\tilde{\phi}_H^{(1)}(x) = \tilde{\Phi}_{c\bar{c}}^{(1)}(x)/\left(\frac{1}{P^z}\bar{u}(p)\gamma^z\Gamma v(p)\right) - \delta\left(x-\frac{1}{2}\right)\mathfrak{f}^{(1)}. \tag{19b}$$

Therefore, we need calculate the order-α_s correction to the partonic (quasi-)DA and corresponding decay constant.

Although LCDAs and quasi-DAs by construction are gauge-invariant objects, practically we have to specify a gauge when computing the one-loop correction. We find it convenient to work with the axial gauges: i.e., $A^+ = 0$ for LCDA and $A^z = 0$ for quasi-DA. In such gauges, the gauge link shrinks to unity, and we have to deal only with a very few diagrams, which are depicted in Fig. 1. Now the complication instead resides in the gluon propagator:

$$D_{\mu\nu}(k) = \frac{-i}{k^2+i\epsilon}\left(g_{\mu\nu} - \frac{n_\mu k_\nu + n_\nu k_\mu}{n\cdot k} + \frac{n^2 k_\mu k_\nu}{n\cdot k^2}\right), \tag{20}$$

where n^μ is defined in (16).

Ultraviolet divergences will inevitably emerge in our calculation, thereby necessitating the introduction of a UV regulator. For the light-cone correlators such as PDF and LCDA, only the logarithmic UV divergences will arise;

nevertheless, for the quasidistributions, one often confronts linear or even more severe UV divergences [14,15]. In order to keep track of these violent UV divergences, it is more transparent to adopt a physical UV regulator such as a hard momentum cutoff than simply use the dimensional regularization (DR). In some sense, the UV cutoff Λ imposed on the transverse-momentum integration may be viewed as intimately mimicking the role placed by the lattice spacing in a lattice Monte Carlo simulation. In this work, we will also utilize the transverse-momentum cutoff Λ to regularize the UV divergence.

Thus far, the renormalization program of nonlocal correlators, particularly the quasidistributions, has not yet been fully developed and remains as an active research topic [15,18]. The hope is that the UV divergences associated with the quasidistributions can be removed through multiplicative renormalization to all orders in α_s [15,18]. As a consequence, a rigorous renormalization procedure of the quasi-DA is beyond the scope of the current work. Our primary goal in this work is to compare the behavior of quasi-DAs and LCDAs at variance with P^z. For this purpose, Λ will be kept finite and taken around the characteristic heavy quark mass scale. Roughly speaking, we pretend to have a "renormalized" LCDA and quasi-DA with Λ interpreted as the corresponding renormalization scale μ in a continuum quantum field theory.

Another practical reason for us to keep Λ finite is because the order of taking two limits $\Lambda \to \infty$ and $P^z \to \infty$ is not commutable. Had $\Lambda \to \infty$ been taken first, the quasidistributions would not approach the light-cone distributions even in the limit $P^z \to \infty$. As the main goal of this paper is to investigate quantitatively how the quasi-DA can approach the LCDA with increasing P^z, therefore, the analytic control of $P^z \to \infty$ limit is a crucial requirement. For this purpose, keeping a finite Λ is crucial.

It is worth pointing out that, besides UV divergences, IR divergences also arise from individual diagrams in Fig. 1. It can be traced from the exchange of a soft gluon between the quark and antiquark that equally partition the total momentum P and so is always accompanied with $\delta(x - \frac{1}{2})$. Of course, when summing the vertex diagram and the quark self-energy diagram together, the IR singularities cancel, as ensured by the validity of NRQCD factorization: the color-singlet NRQCD bilinears such as $\psi^\dagger\chi$ and $\psi^\dagger\boldsymbol{\sigma}\chi$ do not acquire an anomalous dimension at the order of α_s.[3] However, it is still necessary to introduce an IR regulator in the intermediate steps. In our calculation, we find it convenient to employ the DR to regularize the IR singularity, working with the spacetime dimension $d = 4 - 2\epsilon$ ($\epsilon < 0$).[4] We stress that the popular way of introducing a fictitious small gluon mass is not sufficient to tame the IR divergences encountered here, because in our calculation the soft IR singularity can be coupled with the axial singularity (stemming from $1/n \cdot k$), where the latter cannot be regularized by just adding m_g alone.[5]

For the one-loop integral, we always choose to first integrate over the k^- (k^0) component using a contour technique for the LCDA (quasi-DA), then carry out the remaining $d-2$-dimensional integration over transverse components, and finally end up with a one-dimensional integral depending on the variable k^+ (k^z) for the LCDA (quasi-DA). Then one can readily read off the desired distribution as a function of x, which is connected with k^+ (k^z) through the relation $k^+ = (x - 1/2)P^+$ [$k^z = (x - 1/2)P^z$] for the LCDA (quasi-DA) that is enforced by the δ function. The following transverse-momentum integration measure is ubiquitously encountered:

$$\left(\frac{\mu_{\rm IR}^2 e^{\gamma_E}}{4\pi}\right)^\epsilon \int d^{2-2\epsilon} k_\perp = \left(\frac{\mu_{\rm IR}^2 e^{\gamma_E}}{4\pi}\right)^\epsilon \frac{2\pi^{1-\epsilon}}{\Gamma(1-\epsilon)} \int_0^\Lambda k_\perp^{1-2\epsilon} dk_\perp, \tag{21}$$

where Λ is the UV cutoff, γ_E is the Euler constant, and $\mu_{\rm IR}$ is the 't Hooft unit mass. We put a subscript "IR" to emphasize that this scale is affiliated with the IR divergence. The main reason why we use DR and a cutoff to regularize IR and UV divergence, respectively, is to ensure that the quasi-DAs reduce to light-cone DAs in the $P^z \gg \Lambda > m$ limit, so that one can investigate the magnitude of P^z needed to recover LCDAs. If the conventional DR is applied, the quasi-DA will equal to the limit $\Lambda \gg P^z > m$ which will not reduce to the LCDA after taking the $P^z \to \infty$ limit. The similar behavior of a quasi-PDF is reported in Refs. [14,15]. We provide a more detailed explanation with an example in Appendix A.

[3] If we attempt to extract the two-loop correction to (quasi-) DAs using the same technique as described in this work, we would confront the uncanceled single IR pole, which should be absorbed into the corresponding vacuum-to-quarkonium NRQCD matrix elements. It is intimately linked to the fact that NRQCD quark bilinears $\psi^\dagger\chi$ and $\psi^\dagger\boldsymbol{\sigma}\chi$ acquire an anomalous dimension first at the order of α_s^2 [38–40].

[4] In a previous calculation of the LCDA of the S-wave quarkonium using NRQCD factorization [28,29], the authors employ the DR to regularize UV and IR divergences simultaneously. If taking $\Lambda \to \infty$ prior to Laurent-expanding ϵ, we would be able to reproduce their unrenormalized one-loop results.

[5] Precisely speaking, the most singular IR behavior is captured by the $\frac{1}{\epsilon_{\rm IR}^2}$ pole if DR is used. If one uses the gluon mass regularization for the soft divergence, one has to invoke an additional regulator such as DR to regularize the axial singularity, so the most severe IR singularity would look like $\frac{1}{\epsilon_{\rm IR}} \ln m_g$ as $x \to \frac{1}{2}$.

For both the LCDA and quasi-DA, the vertex diagram in Fig. 1 can be written as

$$\Phi_{c\bar{c}}^{(1)\,\mathrm{ver}} = g_s^2 C_F \left(\frac{\mu_{\mathrm{IR}}^2 e^{\gamma_E}}{4\pi}\right)^{\epsilon} \int \frac{d^{4-2\epsilon}k}{(2\pi)^{4-2\epsilon}} \bar{u}(p)\gamma^\mu \frac{1}{\not{k}+\not{p}-m+i\epsilon} \not{n}\{\gamma^5, \mathbf{1}, \gamma^\perp\} \times \frac{1}{\not{k}-\not{p}-m+i\epsilon}\gamma^\nu v(p) D_{\mu\nu}(k)\delta\left(x-\frac{1}{2}-\frac{n\cdot k}{n\cdot P}\right). \tag{22}$$

The three terms associated with the gluon propagator have a one-to-one correspondence with what would be encountered in a Feynman-gauge calculation. The second and third terms correspond to the diagrams entailing a gauge-link interaction. Particularly, the third term will correspond to a self-energy correction to the gauge link and would actually lead to a linear UV divergence for the quasi-DA.

In Appendix B, we have provided comprehensive details on how to work out the Feynman part ($\propto g_{\mu\nu}$ in the gluon propagator) of this one-loop vertex integral. After accomplishing all the algebra, it is reassuring that $\Phi_{c\bar{c}}^{(1)\,\mathrm{ver}}$ turns out to possess exactly the same Lorentz structure as the tree-level format, $\propto \frac{1}{P^+}\bar{u}(p)\gamma^+\Gamma v(p)$. This feature is in conformity with Eq. (19).

According to the Lehmann-Symanzik-Zimmermann reduction formula, we also have to include the order-α_s correction to the quark wave function renormalization constant. It yields only a $\delta(x-\frac{1}{2})$ piece to $\Phi_{c\bar{c}}(x)$ [$\tilde{\Phi}_{c\bar{c}}(x)$]. The contributions from the last two diagrams in Fig. 1 read

$$\Phi_{c\bar{c}}^{(1)\,\mathrm{wvf}} = \frac{1}{2}[\delta Z_{F,q}^{(1)} + \delta Z_{F,\bar{q}}^{(1)}]\delta\left(x-\frac{1}{2}\right), \tag{23a}$$

$$\tilde{\Phi}_{c\bar{c}}^{(1)\,\mathrm{wvf}} = \frac{1}{2}[\delta \tilde{Z}_{F,q}^{(1)} + \delta \tilde{Z}_{F,\bar{q}}^{(1)}]\delta\left(x-\frac{1}{2}\right). \tag{23b}$$

The quark wave function renormalization constant Z_F in axial gauges is considerably more complicated than its counterpart in covariant gauges.

We follow the recipe given in Ref. [14] to express them as

$$\delta Z_q = \bar{u}(p)\frac{\partial\Sigma(p)}{\partial(n\cdot p)}u(p)/[\bar{u}(p)\not{n}u(p)], \tag{24a}$$

$$\delta Z_{\bar{q}} = \bar{v}(p)\frac{\partial\Sigma(p)}{\partial(n\cdot p)}v(p)/[\bar{v}(p)\not{n}v(p)]. \tag{24b}$$

At the order of α_s, they read

$$\delta Z_q^{(1)} = -C_F g_s^2 \left(\frac{\mu_{\mathrm{IR}}^2 e^{\gamma_E}}{4\pi}\right)^{\epsilon} \int \frac{d^{4-2\epsilon}k}{(2\pi)^{4-2\epsilon}} \bar{u}(p)\frac{1}{\not{k}+\not{p}-m+i\epsilon}\not{n} \times \frac{1}{\not{k}+\not{p}-m+i\epsilon}u(p)D_{\mu\nu}(k)/[\bar{u}(p)\not{n}u(p)], \tag{25a}$$

$$\delta Z_{\bar{q}}^{(1)} = -C_F g_s^2 \left(\frac{\mu_{\mathrm{IR}}^2 e^{\gamma_E}}{4\pi}\right)^{\epsilon} \int \frac{d^{4-2\epsilon}k}{(2\pi)^{4-2\epsilon}} \bar{v}(p)\frac{1}{\not{k}-\not{p}-m+i\epsilon}\not{n} \times \frac{1}{\not{k}-\not{p}-m+i\epsilon}v(p)D_{\mu\nu}(k)/[\bar{v}(p)\not{n}v(p)]. \tag{25b}$$

The detailed derivation of their analytic expressions is also presented in Appendix B.

Both the vertex diagram and self-energy diagrams contain IR divergences. After some manipulations as elaborated in Appendix B, we are able to isolate those IR-divergent parts as the terms containing $(1-2x)^{-1-2\epsilon}$ and $(1-2x)^{-2-2\epsilon}$. With the aid of the distribution identities listed in Appendix C, we can rewrite these terms as the IR pole of the form $\delta(x-1/2)/\epsilon_{\mathrm{IR}}$ and the plus (double-plus) functions. The "+" and "++" functions are distributions, in the sense that when convoluted with a test function $g(x)$, they give

$$\int_0^{\frac{1}{2}} dx[f(x)]_+ g(x) = \int_0^{\frac{1}{2}} dx f(x)\left[g(x)-g\left(\frac{1}{2}\right)\right], \tag{26a}$$

$$\int_0^{\frac{1}{2}} dx[f(x)]_{++} g(x) = \int_0^{\frac{1}{2}} dx f(x)\left[g(x)-g'\left(\frac{1}{2}\right)\left(x-\frac{1}{2}\right)-g\left(\frac{1}{2}\right)\right], \tag{26b}$$

where $g(x)$ is regular at $x=1/2$. The above two definitions are also valid if we replace the integration range from $0\le x\le 1/2$ to $1/2\le x\le 1$.

Upon summing the vertex and self-energy diagrams, all the double and single IR poles cancel, and we are left with regular (at $x=1/2$) functions as well as plus distributions. After some reshuffling of terms, we are able to rewrite $\Phi_{c\bar{c}}^{(1)}(x)$ [$\tilde{\Phi}_{c\bar{c}}^{(1)}(x)$] as an entire ++ function plus an IR-finite piece proportional to $\delta(x-\frac{1}{2})$.

The partonic DA $\Phi^{(1)}(x)$ is not the desired short-distance distribution. In compliance with (19), we have to subtract the order-α_s correction to the decay constant in order to acquire the normalized LCDA and quasi-DA. It is straightforward to compute the order-α_s correction to the decay constants associated with various S-wave quarkonia:

$$\mathfrak{f}_{\eta_c}^{(1)} = -1 - \frac{\Lambda}{m}\tan^{-1}\left(\frac{m}{\Lambda}\right) + \frac{\Lambda^2}{2m^2}\ln\left(\frac{\Lambda^2+m^2}{\Lambda^2}\right), \quad (27a)$$

$$\mathfrak{f}_{J/\psi}^{\parallel(1)} = -1 - \left(\frac{\Lambda}{m}+\frac{m}{\Lambda}\right)\tan^{-1}\left(\frac{m}{\Lambda}\right), \quad (27b)$$

$$\mathfrak{f}_{J/\psi}^{\perp(1)} = -1 - \left(\frac{\Lambda}{m}+\frac{m}{\Lambda}\right)\tan^{-1}\left(\frac{m}{\Lambda}\right) + \frac{\Lambda^2+m^2}{4m^2}\ln\left(\frac{\Lambda^2+m^2}{m^2}\right) - \frac{\Lambda^2}{2m^2}\ln\left(\frac{\Lambda}{m}\right). \quad (27c)$$

Again we have kept a finite Λ but take the IR regulator $\epsilon \to 0$, since they are IR finite. For the η_c and $J/\psi^{\parallel}$, the one-loop corrections are UV finite, and our results agree with the existing results in literature once taking $\Lambda \to \infty$. For $J/\psi^{\perp}$, the order-α_s correction is logarithmically UV-divergent, and our result agrees with the existing results that employ the DR as a UV regulator but differs in the finite piece.

Not surprisingly, after incorporating the very one-loop corrections to the decay constants in (27), the extra $\delta(x-\frac{1}{2})$ pieces in $\Phi^{(1)}(x)$ get exactly canceled in (19). We thereby obtain the properly normalized $\phi_H^{(1)}(x)$ $[\tilde{\phi}_H^{(1)}(x)]$, in the sense that $\int_0^1 dx\phi_H^{(1)}(x) = \int_{-\infty}^{\infty} dx\tilde{\phi}_H^{(1)}(x) = 0$.

D. Analytic expressions of order-α_s LCDA and DA of S-wave quarkonia

In this section, we present the analytical expressions for the order-α_s corrections to the DAs of various helicity states of S-wave quarkonia.

The LCDAs of three S-wave quarkonium states have a rather quite compact form:

$$\phi_{\eta_c}^{(1)}(x;\Lambda,m) = \left[x\left(\frac{2}{1-2x}+1\right)\log\left(\frac{\Lambda^2}{m^2(1-2x)^2}+1\right) + \frac{2x\Lambda^2}{(1-2x)^2(\Lambda^2+m^2(1-2x)^2)} + (x\to 1-x)\right]_{++}, \quad (28a)$$

$$\phi_{J/\psi}^{\parallel,(1)}(x;\Lambda,m) = \left[x\left(\frac{2}{1-2x}+1\right)\log\left(\frac{\Lambda^2}{m^2(1-2x)^2}+1\right) + \frac{8x^2(1-x)\Lambda^2}{(1-2x)^2(\Lambda^2+m^2(1-2x)^2)} + (x\to 1-x)\right]_{++}, \quad (28b)$$

$$\phi_{J/\psi}^{\perp,(1)}(x;\Lambda,m) = \left[\frac{2x}{1-2x}\log\left(\frac{\Lambda^2}{m^2(1-2x)^2}+1\right) + \frac{2x\Lambda^2}{(1-2x)^2(\Lambda^2+m^2(1-2x)^2)} + (x\to 1-x)\right]_{++}, \quad (28c)$$

all of which have support only in the range $0 \le x \le 1$. These LCDAs are symmetric under $x \leftrightarrow 1-x$, as demanded by charge conjugation symmetry.

Note that all these LCDAs contain explicit $\ln\Lambda$ dependence. This is in conformity with the celebrated Efremov-Radyushkin-Brodsky-Lepage (ERBL) evolution equation [41,42]:

$$\frac{d}{d\ln\Lambda^2}\Phi_H(x;\Lambda) = \frac{\alpha_s C_F}{\pi}\int_0^1 dy V_0(x,y)\Phi_H(y,\Lambda) + \mathcal{O}(\alpha_s^2), \quad (29)$$

where the evolution kernel $V_0(x,y)$ varies with different hadron helicity. Substituting the $\phi_H^{(1)}$ in (28) back to (7a) and plugging into (29), also taking into account the order-α_s correction to the decay constant in (27), it is straightforward to check that all of these LCDAs indeed obey the ERBL equation.

Conceivably, the nonlogarithm terms in (28) differ from those given in [29],[6] which can be attributed to the different choice of UV regulators. Had we first sent $\Lambda \to \infty$ during the intermediate stage, which amounts to using DR to regulate both UV and IR divergences, we would be able to reproduce their results.

[6]When computing the order-α_s correction to the color-singlet channel of the double parton fragmentation function, the corresponding results in Ref. [43] are equivalent to those of the LCDA [29].

Next we turn to the quasi-DA. Since the boost invariance is sacrificed there, the expressions would explicitly depend on P^z and, consequently, become considerably more complicated:

$$\begin{aligned}\tilde{\phi}^{(1)}_{\eta_c}(x,P^z;\Lambda,m) = \Bigg[& -x\left(1+\frac{2}{1-2x}\right)\frac{p^z}{p^0}\ln\left(\frac{p^0\sqrt{\Lambda^2+m^2+4(p^z)^2x^2}+2(p^z)^2x+m^2}{p^0\sqrt{m^2+4(p^z)^2x^2}+2(p^z)^2x+m^2}\right) \\ & +\frac{(1-x)p^z}{p^0}\ln\left(\frac{(1-2x)(p^z)^2+\sqrt{\Lambda^2+(-1+2x)^2(p^z)^2}p^0}{(1-2x)(p^z)^2+p^z\sqrt{(p^z)^2+m^2}|1-2x|}\right) \\ & -\frac{2(1-x)p^z}{(1-2x)p^0}\ln\left(\frac{\sqrt{(\Lambda^2+(1-2x)^2(p^z)^2)}p^0+(1-2x)(p^z)^2}{|1-2x|p^zp^0+(1-2x)(p^z)^2}\right) \\ & +\frac{(\Lambda^2(p^0)^2-2m^2x(1-2x)(p^z)^2)\sqrt{\Lambda^2+4x^2(p^z)^2+m^2}}{2(m^2(1-2x)^2(p^z)^2+\Lambda^2(p^0)^2)(1-2x)p^z}+\frac{x\sqrt{4x^2(p^z)^2+m^2}}{(1-2x)^2p^z} \\ & +\frac{m^2p^z\sqrt{\Lambda^2+(1-2x)^2(p^z)^2}}{2(\Lambda^2+(1-2x)^2(p^z)^2)m^2+2\Lambda^2(p^z)^2}+\frac{\sqrt{\Lambda^2+(1-2x)^2(p^z)^2}}{2(1-2x)^2p^z}-\frac{1}{|1-2x|}+(x\to 1-x)\Bigg]_{++},\end{aligned} \tag{30a}$$

$$\begin{aligned}\tilde{\phi}^{\parallel,(1)}_{J/\psi}(x,P^z;\Lambda,m) = \Bigg[& \left(\frac{p^z(m^2+2x(p^z)^2)}{2(p^0)^3}+\frac{p^z(m^2(2x+1)+4x(p^z)^2)}{2(1-2x)(p^0)^3}\right)\ln\left(\frac{p^0\sqrt{m^2+\Lambda^2+4x^2(p^z)^2}-m^2-2x(p^z)^2}{p^0\sqrt{m^2+4x^2(p^z)^2}-m^2-2x(p^z)^2}\right) \\ & +\left(\frac{(1-2x)(p^z)^3}{2(p^0)^3}-\frac{p^z(m^2(2x+1)+4x(p^z)^2)}{2(1-2x)(p^0)^3}\right)\ln\left(\frac{p^0\sqrt{\Lambda^2+(1-2x)^2(p^z)^2}+(1-2x)(p^z)^2}{p^zp^0|1-2x|+(1-2x)(p^z)^2}\right) \\ & -\frac{p^z}{4p^0}\log\left(\frac{\Lambda^2(p^0)^2}{m^2(p^z)^2(1-2x)^2}+1\right)+\frac{(m^2+4(1-x)x(p^z)^2)(\sqrt{m^2+4x^2(p^z)^2}-|1-2x|p^z)}{2(1-2x)^2p^z(p^0)^2} \\ & +\frac{m^2p^z(m^2-4(x-1)x(p^z)^2)(\sqrt{\Lambda^2+(1-2x)^2(p^z)^2}-\sqrt{m^2+\Lambda^2+4x^2(p^z)^2})}{2(p^0)^2(m^2(\Lambda^2+(1-2x)^2(p^z)^2)+\Lambda^2(p^z)^2)} \\ & +\frac{p^z(\sqrt{m^2+\Lambda^2+4x^2(p^z)^2}-\sqrt{m^2+4x^2(p^z)^2})}{2(1-2x)(p^0)^2}+\frac{\sqrt{\Lambda^2+(1-2x)^2(p^z)^2}}{2(1-2x)^2p^z}-\frac{1}{2|1-2x|}+(x\to 1-x)\Bigg]_{++},\end{aligned} \tag{30b}$$

$$\begin{aligned}\tilde{\phi}^{\perp,(1)}_{J/\psi}(x,P^z;\Lambda,m) = \Bigg[& -\frac{p^z}{p^0}\ln\left(\frac{p^0\sqrt{\Lambda^2+(1-2x)^2(p^z)^2}+(1-2x)(p^z)^2}{p^zp^0|1-2x|+(1-2x)(p^z)^2}\right) \\ & -\frac{2xp^z}{p^0}\ln\left(\frac{p^0\sqrt{\Lambda^2+m^2+4(p^z)^2x^2}+2(p^z)^2x+m^2}{p^0\sqrt{m^2+4(p^z)^2x^2}+2(p^z)^2x+m^2}\right)-\frac{p^z}{2p^0}\ln\left(\frac{\Lambda^2(p^0)^2}{m^2(1-2x)^2(p^z)^2}+1\right) \\ & +\frac{\sqrt{\Lambda^2+m^2+4x^2(p^z)^2}}{2(1-2x)p^z}-\frac{m^2p^z\sqrt{\Lambda^2+m^2+4x^2(p^z)^2}}{2m^2(p^z)^2(1-2x)^2+2(p^0)^2\Lambda^2}+\frac{x\sqrt{m^2+4x^2(p^z)^2}}{p^z(1-2x)^2}-\frac{1}{|1-2x|} \\ & +\frac{m^2p^z\sqrt{\Lambda^2+(1-2x)^2(p^z)^2}}{2(m^2(p^z)^2(1-2x)^2+(p^0)^2\Lambda^2)}+\frac{\sqrt{\Lambda^2+(1-2x)^2(p^z)^2}}{2(1-2x)^2p^z}+(x\to 1-x)\Bigg]_{++},\end{aligned} \tag{30c}$$

where $p^0 \equiv \sqrt{(p_z)^2+m^2}$. Needless to say, these quasi-DAs are also symmetric under the transformation $x \leftrightarrow 1-x$.

A major difference between quasi-DAs and LCDAs is that the former have a nonvanishing support when $x<0$ and $x>1$, though suppressed by $1/(P^z)^2$. This is a general feature of quasidistributions, which was also seen in the quasi-PDF and generalized parton distribution. This simply signals the breakdown of a physical parton interpretation for quasidistributions.

Reassuringly, it can be analytically checked, when boosted to the IMF by sending $P^z\to\infty$, that these

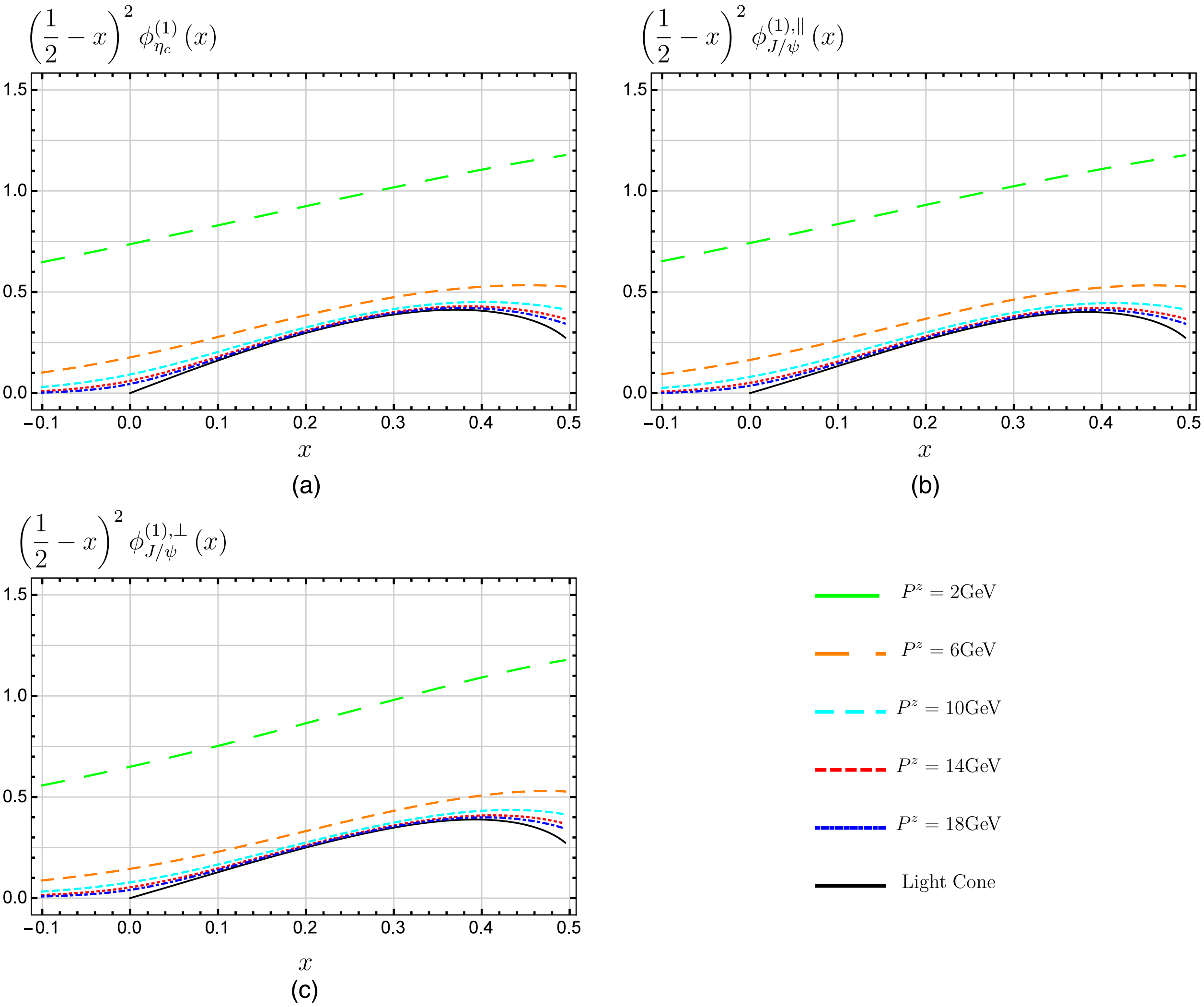

FIG. 2. LCDAs and quasi-DAs for three S-wave charmonium helicity states with various P^z.

frame-dependent quasi-DAs in (30) indeed reduce to the exact functional form of the LCDAs in (28).

Note that all the $\tilde{\phi}_H^{(1)}(x)$ in (28) contain a linearly UV-divergent piece $\sqrt{\Lambda^2 + (1-2x)^2(p^z)^2}$. This term is always accompanied with the double pole $(1-2x)^{-2}$ and suppressed by $1/P^z$. Physically, such a term can be traced to the self-energy correction to the gauge link. In this work, we have keep Λ finite, so such a term does not bring any problem. For a consistent renormalization program, the proper treatment of such a term in the limit $\Lambda \to \infty$ at fixed P^z has been sketched in Refs. [14,16].

Had we taken the $\Lambda \gg P^z \gg m$ limit in the quasi-DA, the BL evolution kernel would also emerge in the range $0 \le x \le 1$, but the accompanied logarithm is in the form of $\ln P^z$ rather than $\ln \Lambda$ as in the LCDA. It is the strength of the recently advocated large momentum effective field theory [11] to resum such a type of logarithms.

IV. NUMERICAL COMPARISON BETWEEN LCDA AND QUASI-DA OF QUARKONIA

Having the one-loop exact "data" available for both the LCDA and quasi-DA of the η_c and J/ψ, it is the time to make a comprehensive study on their properties.

A. The convergence behavior of quasi-DAs to LCDAs with increasing P^z

We have already seen that the quasi-DAs in the limit $P^z \to \infty$ analytically recover the LCDAs for each species of quarkonia. It is of practical curiosity to see explicitly how fast the quasi-DA approaches the LCDA with increasing P^z.

For numerical study, we take the charm quark mass as 1.4 GeV. We tentatively choose $\Lambda = 3$ GeV, approximately equal to the masses of η_c and J/ψ. In Fig. 2, for each species of S-wave charmonia, we display several sets of the quasi-DAs at various values of P^z: 2, 6, 10, 14, and 18 GeV, respectively. Because the DAs are symmetric under

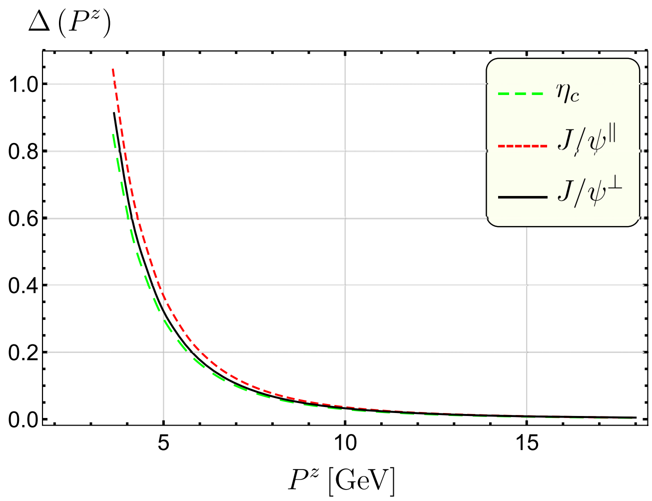

FIG. 3. The degree of resemblance as a function of P^z.

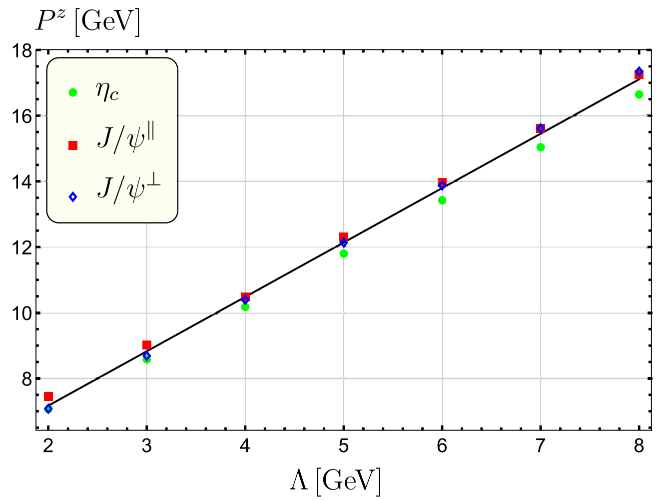

FIG. 4. To fulfill $\Delta = 0.05$, the minimal value of P^z required as a function of Λ.

$x \leftrightarrow 1-x$, and quasi-DAs decrease very rapidly in the unphysical regions $x<0$ and $x>1$, we plot them only in the interval $-0.1<x<1/2$. In order to suppress the singular appearance near $x \sim \frac{1}{2}$, we deliberately multiply all the DAs by $(1-2x)^2$.

From Fig. 2, we clearly see the trend of the quasi-DA approaching the LCDA with increasing P^z. Also, it is interesting to note that the quasi-DA admits a nonzero value at $x=0$ and 1, which is quite different from the LCDA.

In order to quantify the difference between the LCDA and quasi-DA at a given P^z, we invent a parameter *degree of resemblance*, denoted by $\Delta(P^z)$:

$$\Delta_H(P^z) = \frac{\int_0^{\frac{1}{2}} dx(1-2x)^4[\phi_H^{(1)}(x;\Lambda,m) - \tilde{\phi}_H^{(1)}(x,P^z;\Lambda,m)]^2}{\int_0^{\frac{1}{2}} dx(1-2x)^4[\phi_H^{(1)}(x;\Lambda,m)]^2}. \tag{31}$$

The dependence of Δ_H on P^z is shown in Fig. 3. It is a rapidly descending function. When P^z is 6 GeV, Δ is about 20%; as P^z is boosted to 9 GeV, Δ already decreases to 5%. It may persuasively imply that, provided that P^z is about 3 times larger than the hadron mass (with the renormalization scale fixed around the hadron mass), the quasi-DA already converges to the "true" LCDA to a decent extent. Interestingly, a very recent investigation on the nucleon quasi-PDF in the diquark model has drawn a similar conclusion [25].

We can further inspect the correlation between P^z and Λ, for a given degree of resemblance. In Fig. 4, we show that, to achieve $\Delta = 0.05$, how the minimal value of P^z required depends on the value of Λ. The colored dots and squares are generated from actual calculations, the solid line is a linear fit by averaging over three types of charmonium helicity states, and we obtain $\bar{P}^z = 1.66\Lambda + 3.86$ GeV. It is interesting to observe this linear correlation between P^z and Λ.

B. Comparison of first inverse moment between LCDA and quasi-DA

In the hard exclusive reactions, the factorization theorem expresses the amplitude as the convolution of the hard-scattering kernel with the LCDAs. For a leading-twist contribution, the hard part always bears the form x^{-1}; thereby, it is the first inverse moment of the LCDA that is of ubiquitous phenomenological interest [44].

We are curious to which extent the inverse moment generated from the quasi-DA will resemble the light-cone one in magnitude. The first inverse moment of the charmonia LCDA, to order-α_s accuracy, is given by

$$\langle x^{-1}\rangle_H \equiv \int_0^1 dx \frac{\phi_H^{(1)}(x;\Lambda,m)}{x}. \tag{32}$$

As dictated by the general principle, $\phi_H \propto x$ as $x \to 0$; thereby, the leading-twist LCDA admits a finite inverse moment. One can readily deduce the closed form for the inverse moments from (28):

$$\langle x^{-1}\rangle_{\eta_c} = -\frac{\pi^2}{6} + \frac{2\Lambda^2 \ln 2}{m^2+\Lambda^2} + \frac{2\Lambda(2m^2+\Lambda^2)}{m(m^2+\Lambda^2)}\arctan\frac{m}{\Lambda} - \ln 2 \ln\frac{\Lambda^2+m^2}{\Lambda^2} + \frac{\Lambda^4+2\Lambda^2m^2+3m^4}{2m^2(\Lambda^2+m^2)}\ln\frac{\Lambda^2+m^2}{\Lambda^2} + (3-2\ln 2)\ln\frac{\Lambda}{m} + 2\mathrm{Re}\left[\mathrm{Li}_2\left(\frac{2m}{m-i\Lambda}\right) - \mathrm{Li}_2\left(\frac{m}{m-i\Lambda}\right)\right], \tag{33a}$$

$$\langle x^{-1}\rangle_{J/\psi^{\parallel}} = -\frac{\pi^2}{6}+\frac{4\Lambda}{m}\arctan\frac{m}{\Lambda}-\frac{\Lambda^2-(3-2\ln 2)m^2}{2m^2}\ln\frac{\Lambda^2+m^2}{\Lambda^2} + (3-2\ln 2)\ln\frac{\Lambda}{m}+2\mathrm{Re}\left[\mathrm{Li}_2\left(\frac{2m}{m-i\Lambda}\right)-\mathrm{Li}_2\left(\frac{m}{m-i\Lambda}\right)\right], \tag{33b}$$

$$\langle x^{-1}\rangle_{J/\psi^{\perp}} = -\frac{\pi^2}{3}+\frac{2\Lambda^2\ln 2}{m^2+\Lambda^2}+\frac{2\Lambda(3m^2+2\Lambda^2)}{m(m^2+\Lambda^2)}\arctan\frac{m}{\Lambda} + 4(1-\ln 2)\ln\frac{\Lambda}{m}-\frac{(2\ln 2-1)\Lambda^2+2(\ln 2-1)m^2}{\Lambda^2+m^2}\ln\frac{\Lambda^2+m^2}{\Lambda^2} + 4\mathrm{Re}\left[\mathrm{Li}_2\left(\frac{2m}{m-i\Lambda}\right)-\mathrm{Li}_2\left(\frac{m}{m-i\Lambda}\right)\right]. \tag{33c}$$

In the $\Lambda \gg m$ limit, the inverse moments are dominated by the $\ln\frac{\Lambda}{m}$ term for each LCDA, whose coefficients agree with the previously known results [29,34]. It is this type of collinear logarithms that can be resummed to orders in α_s with the aid of the ERBL evolution equation [33].

In contrast, as can be analytically inferred from (30) or clearly seen from Fig. 2, the quasi-DAs approach nonzero values as $x \to 0$. Nevertheless, the quasi-DAs still smoothly cross $x = 0$; we thus utilize the principal value prescription to define the inverse moment of the quasi-DA:

$$\langle \tilde{x}^{-1}\rangle_H \equiv \mathrm{P.V.}\int_{-\infty}^{\infty} dx\frac{\tilde{\phi}_H^{(1)}(x,P^z;\Lambda,m)}{x}. \tag{34}$$

The magnitudes of the first inverse moments of the LCDA and quasi-DA as a function of P^z are presented in Fig. 5, with Λ fixed at 3 GeV. To characterize the extent of the proximity of the first inverse moments between the LCDA and quasi-DA, we introduce the following fractional difference:

$$\Omega_H(P^z,\Lambda) = \left|\frac{\langle x^{-1}\rangle_H - \langle \tilde{x}^{-1}\rangle_H}{\langle x^{-1}\rangle_H}\right|. \tag{35}$$

Concretely speaking, at $\Lambda = 3$ GeV, the Ω_H for three types of S-wave states are shown in Table I We see that, even when P^z is boosted to 9 GeV, the inverse moments generated from the quasi-DA still differ from the true results by about 20%. Compared with $\Delta_H(P^z)$, the first inverse moments generated by the quasi-DAs appear to approach the LCDA value with a rather slower pace.

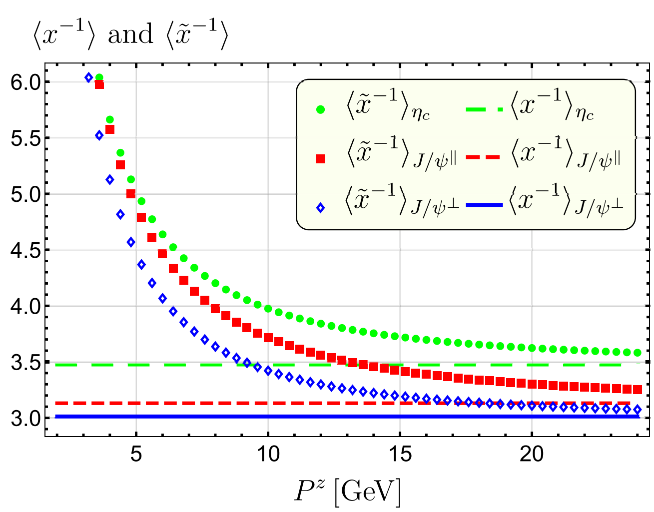

FIG. 5. The first inverse moments obtained from various S-wave quarkonia, for both order-α_s LCDA and quasi-DA, as a function of P^z. We fix $\Lambda = 3$ GeV.

V. SUMMARY

The PDF and LCDA are among the most prominent and basic nonperturbative quantities coined in QCD, encapsulating rich dynamics about the quark-gluon degree of freedom inside a hadron. For several decades, how to effectively compute such light-cone distributions from the first principle of QCD has posed a preeminent challenge, and progress was slow. As a breakthrough, the recently advocated quasidistributions, and the corresponding large momentum effective field theory, have the very bright prospect to help finally overcome this long-standing difficulty.

Despite some important progress, there remain eminent technical obstacles for the lattice to make phenomenologically competitive measurements on quasidistributions. One is the lack of a systematic renormalization program for quasidistributions. Moreover, for the current lattice technique, to make a precise simulation for quasidistributions in

TABLE I. Numerical results of Ω_{η_c}, $\Omega_{J/\psi^{\parallel}}$ and $\Omega_{J/\psi^{\perp}}$ with different hadrons' momenta.

P^z	Ω_{η_c}	$\Omega_{J/\psi^{\parallel}}$	$\Omega_{J/\psi^{\perp}}$
6 GeV	0.335	0.431	0.358
9 GeV	0.172	0.228	0.174
18 GeV	0.052	0.071	0.049

a highly boosted hadron state is also unrealistic. Therefore, it is valuable if some useful insights about the general aspects of quasidistributions can be gained in the continuum field theory.

Thank to its tremendous simplicity, heavy quarkonium actually provides an ideal theoretical laboratory to study quasidistributions. It has been known that NRQCD factorization allows one to express the LCDA of a heavy quarkonium, at the lowest order in velocity expansion, simply as the product of a perturbatively calculable, IR-finite coefficient function and a single nonperturbative matrix element. Therefore, the profile of the quarkonium LCDA is fully amenable to the perturbation theory. Quarkonium thus constitutes a rare example that the light-cone correlators can be fairly well understood in the continuum theory without much effort.

In this work, extending the previous work on quarkonium LCDAs, we apply NRQCD factorization further to the quasi-DA of the ground-state quarkonia and calculate the respective coefficient functions to order α_s. We are able to show analytically that the quasi-DA exactly reduces into the LCDA in the infinity-momentum limit. We also observe that, provided that the P^z of a charmonium is about 2–3 times its mass and with the renormalization scale chosen around the charmonium mass, the respective quasi-DAs will converge to the LCDAs to a satisfactory degree.

Our work also has some limitation, chiefly in that we have resided entirely in a cutoff theory and naively interpreted the hard transverse-momentum cutoff Λ as the renormalization scale. It is worth pursuing the rigorous renormalization procedure to the quasi-DAs in future work.

We hope our comprehensive study of the quasi-DAs for heavy quarkonia will provide some useful guidance to the future lattice investigation of similar quasidistributions, e.g., how to optimally choose the parameters in their Monte Carlo simulation.

ACKNOWLEDGMENTS

We thank Deshan Yang for useful discussions. The work of Y. J. is supported in part by the National Natural Science Foundation of China under Grants No. 11475188 and No. 11261130311 (CRC110 by DGF and NSFC), by the IHEP Innovation Grant under Contract No. Y4545170Y2, and by the State Key Lab for Electronics and Particle Detectors.

APPENDIX A: COMPARISON BETWEEN DR+CUTOFF REGULARIZATION AND DR REGULARIZATION

The most important reason we use DR and cutoff regularization simultaneously is to justify taking the $P^z \gg \Lambda$, m limit of the quasi-DA to reduce to the LCDA. In the conventional dimensional regularization, the renormalization scale is an overall factor as

$$\left(\frac{\mu^2 e^\gamma}{4\pi}\right)^\epsilon \int \frac{d^{4-2\epsilon}k}{(2\pi)^{4-2\epsilon}} \mathcal{I}(k^\mu, P^z, m). \tag{A1}$$

The $\mu \to \infty$ and $P^z \to \mu$ limits are independent, and the latter one of the quasi-DA does not reduce to the LCDA. We demonstrate the difference between conventional DR regularization and DR + cutoff regularization with the following integral:

$$f_n(x) = \left(\frac{\mu^2 e^\gamma}{4\pi}\right)^\epsilon \int \frac{d^{4-2\epsilon}k}{(2\pi)^{4-2\epsilon}} \frac{1}{(k^2 - m^2 + i\epsilon)[(P-k)^2 + i\epsilon]} \delta\left(x - \frac{n\cdot k}{n\cdot P}\right), \tag{A2}$$

where $n^\mu = (1, \mathbf{0}^\perp, -1)/\sqrt{2}$ for the light-cone case and $n^\mu = (0, \mathbf{0}^\perp, -1)$ for the quasi case. The light-cone integral can be calculated using light-cone coordinates and integrating $\boldsymbol{k}^\perp$ without a cutoff (from $-\infty$ to ∞):

$$f(x,\mu) = \begin{cases} \frac{i}{16\pi^2} \frac{e^{\epsilon\gamma}\mu^{2\epsilon}\csc(\pi\epsilon)}{\Gamma(1-\epsilon)m^{2\epsilon}(1-x)^{2\epsilon}} & 0 < x < 1, \\ 0 & \text{otherwise.} \end{cases} \tag{A3}$$

After $\epsilon \to 0$ expansion we have

$$f(x) = \begin{cases} \frac{i}{16\pi^2}\left[\frac{1}{\epsilon} + \ln\frac{\mu^2}{m^2} - 2\ln(1-x)\right] & 0 < x < 1, \\ 0 & \text{otherwise.} \end{cases} \tag{A4}$$

The ϵ^{-1} will be dropped after renormalization.

For the quasi-integral, integrating out $\boldsymbol{k}^{\perp}$ without a cutoff (from $-\infty$ to ∞) gives

$$\begin{aligned}\tilde{f}(x,P^z,\mu)=&\frac{i2^{\frac{1}{2}-\epsilon}\Gamma(\frac{1}{2}+\epsilon)e^{\gamma\epsilon}\mu^{2\epsilon}(P^z)^{1-2\epsilon}}{16\pi^2\sqrt{\pi}(1-2\epsilon)(P^0)^2}\left[(-P^z\mathrm{sgn}(1-x)+im)\left(\frac{-iP^z\mathrm{sgn}(1-x)+m}{m}\right)^{\frac{1}{2}+\epsilon}\right.\\&\times{}_2F_1\left(\frac{1}{2}-\epsilon,\frac{1}{2}+\epsilon,\frac{3}{2}-\epsilon,\frac{iP^z\mathrm{sgn}(1-x)+m}{2m}\right)|1-x|^{-2\epsilon}\\&-(P^z)^{2\epsilon}\left(imP^z|1-x|^{\frac{1}{2}-\epsilon}+(m^2+(P^z)^2x)|1-x|^{-\frac{1}{2}-\epsilon}\right)\\&\left.\times{}_2F_1\left(\frac{1}{2}-\epsilon,\frac{1}{2}+\epsilon,\frac{3}{2}-\epsilon,\frac{mP^z|1-x|-i(P^0)^2}{2mP^z|1-x|}\right)\right],\end{aligned}\tag{A5}$$

where $P^0=\sqrt{(P^z)^2+m^2}$ and $\mathrm{sgn}(x)$ is the sign function. After $\epsilon\to 0$ expansion we have

$$\begin{aligned}\tilde{f}(x,P^z,\mu)=&\frac{i}{16\pi^2}\frac{P^z}{P^0}\ln\left[(P^z\mathrm{sgn}(1-x)+\sqrt{m^2+(P^z)^2\mathrm{sgn}^2(1-x)})P^0P^z\sqrt{m^2+(P^z)^2x^2}|1-x|\right.\\&\left.\times(m^4-(P^z)^2x(P^0\sqrt{m^2+(P^z)^2x^2}-(P^z)^2x)+m^2((P^z)^2(1+x^2)-P^0\sqrt{m^2+(P^z)^2x^2}))^{-1}\right].\end{aligned}\tag{A6}$$

Taking the limit $P^z\to\infty$ gives

$$\lim_{P^z\to\infty}\tilde{f}(x,P^z,\mu)=\frac{i}{16\pi^2}\begin{cases}\ln\frac{x-1}{x} & x<0,\\ \ln\frac{(P^z)^2}{m^2}+\ln\frac{4x}{1-x} & 0<x<1,\\ \ln\frac{x}{x-1} & x>1,\end{cases}\tag{A7}$$

which does not recover the light-cone integral in Eq. (A4).

If we apply a transverse-momentum cutoff to the loop integral

$$\int d^{4-2\epsilon}k\to\begin{cases}\int_{-\infty}^{\infty}dk^-\int_{-\infty}^{\infty}dk^+\int_0^{\Lambda^2}d(k_\perp^2)(k_\perp^2)^{-\epsilon} & \text{light-cone},\\ \int_{-\infty}^{\infty}dk^0\int_{-\infty}^{\infty}dk^z\int_0^{\Lambda^2}d(k_\perp^2)(k_\perp^2)^{-\epsilon} & \text{quasi},\end{cases}\tag{A8}$$

we will have (after $\epsilon\to 0$ expansion) the light-cone integral

$$f(x,\Lambda)=\begin{cases}\frac{i}{16\pi^2}\ln\frac{\Lambda^2+m^2(1-x)^2}{m^2(1-x)^2} & 0<x<1\\ 0 & \text{otherwise}\end{cases}\tag{A9}$$

and quasi-integral

$$\begin{aligned}\tilde{f}(x,\Lambda)=&\frac{i}{32\pi^2}\frac{P^z}{P^0}\left[\mathrm{sgn}(x(P^z)^2+m^2)\ln\frac{|m^2+x(P^z)^2|+P^0\sqrt{x^2(P^z)^2+m^2}}{|m^2+x(P^z)^2|+P^0\sqrt{x^2(P^z)^2+m^2+\Lambda^2}}\right.\\&+\mathrm{sgn}(x(P^z)^2+m^2)\ln\frac{|m^2+x(P^z)^2|-P^0\sqrt{x^2(P^z)^2+m^2+\Lambda^2}}{|m^2+x(P^z)^2|-P^0\sqrt{x^2(P^z)^2+m^2}}\\&\left.+\mathrm{sgn}(1-x)\ln\frac{(P^0-P^z)(P^0|1-x|\sqrt{\Lambda^2+(1-x)^2(P^z)^2}-(1-x)^2(P^z)^2)}{(P^0+P^z)(P^0|1-x|\sqrt{\Lambda^2+(1-x)^2(P^z)^2}+(1-x)^2(P^z)^2)}\right].\end{aligned}\tag{A10}$$

It is straightforward to check that the $P^z\gg\Lambda$, m limit recovers the light-cone integral (with cutoff) result in Eq. (A9):

$$\lim_{P^z\to\infty}\tilde{f}(x,P^z,\mu)=f(x,\Lambda)=\begin{cases}\frac{i}{16\pi^2}\ln\frac{\Lambda^2+m^2(1-x)^2}{m^2(1-x)^2} & 0<x<1,\\ 0 & \text{otherwise.}\end{cases}\tag{A11}$$

The above example has shown that the integral with a transverse-momentum cutoff reduces to the light-cone result when taking the $P^z \gg \Lambda$, m limit, while taking the $\Lambda \gg P^z$, m limit, which corresponds to conventional DR, does not reduce to the light-cone result.

APPENDIX B: DETAILS OF CONDUCTING THE ONE-LOOP CALCULATION

It is easiest to compute the order-α_s correction to DAs of the longitudinally polarized J/ψ. Therefore, in this section, we take the Feynman part [the $g_{\mu\nu}$ part in the gluon propagator in (20)] as a concrete example to illustrate the intermediate steps in the one-loop calculation for the LCDA and quasi-DA of $J/\psi^{\parallel}$.

1. LCDA

For the LCDA of $J/\psi^{\parallel}$, we take n^μ as the lightlike reference vector defined in (16). The Feynman part of the vertex diagram in (22) reads

$$\begin{aligned}\mathcal{I}(x)=&\frac{C_F}{(2\pi)^{4-2\epsilon}}\left(\frac{\mu_{\rm IR}^2e^{\gamma_E}}{4\pi}\right)^{\epsilon}\int d^dk\bar{u}(p)(-ig_s\gamma^\mu)\frac{i}{\not p+\not k-m+i\epsilon}\gamma^+\frac{i}{\not p-\not k-m+i\epsilon}\\&\times(-ig_s\gamma^\nu)v(p)\frac{-ig_{\mu\nu}}{k^2+i\epsilon}\delta\left(x-\frac{1}{2}-\frac{k^+}{2p^+}\right)/\bar{u}(p)\gamma^+v(p)\\&\times\frac{-ig_s^2C_F}{(2\pi)^{4-2\epsilon}}\left(\frac{\mu_{\rm IR}^2e^{\gamma_E}}{4\pi}\right)^{\epsilon}\frac{2\pi^{1-\epsilon}}{\Gamma(1-\epsilon)}\int_0^\Lambda dk_\perp k_\perp^{1-2\epsilon}\int dk^-dk^+\\&\times\frac{-4(1-\epsilon)k_\perp^2+\frac{8p^-}{p^+}(k^+)^2-8m^2}{[2(k^-+p^-)(k^++p^+)-k_\perp^2-m^2+i\epsilon][2(k^--p^-)(k^+-p^+)-k_\perp^2-m^2+i\epsilon]}\\&\times\frac{\delta(x-\frac{1}{2}-\frac{k^+}{2p^+})\bar{u}(p)\gamma^+v(p)}{2k^-k^+-k_\perp^2+i\epsilon}.\end{aligned}\tag{B1}$$

The k^- integral is carried out by contour integration. The δ function trades the k^+ in favor of the dimensionless momentum fraction x. As is well known, the $\mathcal{I}(x)$ vanishes unless $0<x<1$, for which the poles are distributed in both the upper and lower half of the complex plane when carrying out the k^- integration. After utilizing Cauchy's theorem, we are left with the integration over the transversa momentum:

$$\begin{aligned}\mathcal{I}(x)=&\frac{g_s^2C_F}{(2\pi)^{3-2\epsilon}}\left(\frac{\mu_{\rm IR}^2e^{\gamma_E}}{4\pi}\right)^{\epsilon}\frac{4\pi^{1-\epsilon}}{\Gamma(1-\epsilon)}\int_0^\Lambda dk_\perp k_\perp^{1-2\epsilon}\theta(x)\theta\left(\frac{1}{2}-x\right)x\\&\times\frac{(1-\epsilon)k_\perp^2+m^2(4(1-\epsilon)x(1-x)+1+\epsilon)}{[k_\perp^2+m^2(1-2x)^2]^2}\\=&\left\{\frac{2\theta(x)\theta(\frac{1}{2}-x)e^{\epsilon\gamma}x(1-\epsilon)^4\Lambda^{4-2\epsilon}\mu_{\rm IR}^{2\epsilon}}{(2-\epsilon)\Gamma(1-\epsilon)(1-2x)^4m^4}\left[(1-\epsilon)_2F_1\left(1,2-\epsilon;3-\epsilon;-\frac{\Lambda^2}{m^2(1-2x)^2}\right)\right.\right.\\&\left.\left.+\frac{(\epsilon-2)m^2(1-2x)^2}{m^2(1-2x)^2+\Lambda^2}\right]\right\}_{1\,\rm st}+\left\{\frac{2\theta(x)\theta(\frac{1}{2}-x)e^{\epsilon\gamma_E}x(4(1-\epsilon)x(1-x)+1+\epsilon)^4\Lambda^{-2\epsilon}\mu_{\rm IR}^{2\epsilon}}{(1-2x)^4}\right.\\&\left.\times\left[\frac{\Lambda^2(1-2x)^2}{(m^2(1-2x)^2+\Lambda^2)\Gamma(1-\epsilon)}+\frac{\epsilon\Lambda^2}{m^2\Gamma(2-\epsilon)}{}_2F_1\left(1,1-\epsilon;2-\epsilon;-\frac{\Lambda^2}{m^2(1-2x)^2}\right)\right]\right\}_{2\,\rm nd}\\&+(x\to1-x).\end{aligned}\tag{B2}$$

For the first piece $\mathcal{I}_1(x)$ (with the subscript "1st"), which originates from the part of the integrand containing $k_\perp^2$, one can safely set $\epsilon\to0$, because it is regular at $x=\frac{1}{2}$. The result is

$$\mathcal{I}_1(x) = \frac{C_F g_s^2}{4\pi^2}\theta(x)\theta\left(\frac{1}{2}-x\right)x\left[\ln\left(1+\frac{\Lambda^2}{m^2(1-2x)^2}\right)-\frac{\Lambda^2}{\Lambda^2+m^2(1-2x)^2}\right]+(x\to 1-x). \tag{B3}$$

The second piece $\mathcal{I}_2(x)$ in (B2) (labeled by the subscript "2nd") turns out to be IR-divergent at $x=\frac{1}{2}$. To isolate the IR pole, we apply the following hypergeometric function ${}_2F_1$ identity:

$$\begin{aligned}{}_2F_1(a,b,c,X) = \frac{\Gamma(c)\pi}{\sin(\pi(b-a))}\Bigg[&\frac{(-X)^{-a}}{\Gamma(b)\Gamma(c-a)\Gamma(a-b+1)}{}_2F_1(a,a-c+1,a-b+1,X^{-1})\\ &-\frac{(-X)^{-b}}{\Gamma(a)\Gamma(c-b)\Gamma(-a+b+1)}{}_2F_1(b,b-c+1,-a+b+1,X^{-1})\Bigg].\end{aligned} \tag{B4}$$

Then the ${}_2F_1$ function in $\mathcal{I}_2$ can be rewritten as

$$\begin{aligned}&{}_2F_1\left(1,1-\epsilon;2-\epsilon;-\frac{\Lambda^2}{m^2(1-2x)^2}\right)\\ &=\pi\csc(\pi\epsilon)\left[\frac{\Gamma(2-\epsilon)}{\Gamma(1-\epsilon)}\left(\frac{|1-2x|m}{\Lambda}\right)^{2-2\epsilon}-\frac{m^2(1-2x)^2\Gamma(2-\epsilon)}{\Lambda^2\Gamma(1-\epsilon)^2\Gamma(\epsilon+1)}{}_2F_1\left(1,\epsilon,\epsilon+1,-\frac{m^2(1-2x)^2}{\Lambda^2}\right)\right].\end{aligned} \tag{B5}$$

Therefore, we have

$$\begin{aligned}\mathcal{I}_2(x) = &\frac{C_F g_s^2}{4\pi^2}\frac{\theta(x)\theta(\frac{1}{2}-x)e^{\epsilon\gamma}x(4(1-\epsilon)x(1-x)+1+\epsilon)\Lambda^{-2\epsilon}\mu_{\mathrm{IR}}^{2\epsilon}}{\Gamma(1-\epsilon)}\\ &\times\left[-\frac{m^2}{m^2(1-2x)^2+\Lambda^2}+\left(\frac{1}{1-2x}\right)^{2+2\epsilon}\left(1+\epsilon\ln\left(\frac{\Lambda^2+m^2(1-2x)^2}{m^2}\right)\right)\right]+\mathcal{O}(\epsilon^1).\end{aligned} \tag{B6}$$

The singular term $(1-2x)^{-2-2\epsilon}$ can be expressed through the distribution identity:

$$\lim_{\epsilon\to 0}\left(\frac{1}{2}-x\right)^{-2-2\epsilon}\to\left(-\frac{1}{2\epsilon}-\log 2\right)\delta'\left(x-\frac{1}{2}\right)-2\delta\left(x-\frac{1}{2}\right)+\left[\frac{1}{(\frac{1}{2}-x)^2}\right]_{++}, \tag{B7}$$

with the single IR pole now manifest. All distribution identities required in this work have been assembled in Appendix C.

Substituting (B7) into (B6) and truncating to the order of ϵ^0, we obtain

$$\begin{aligned}\mathcal{I}_2(x) = \frac{C_F g_s^2}{4\pi^2}\Bigg\{&\frac{1}{8}\delta'\left(x-\frac{1}{2}\right)\left[-x(1-2x)^2-\frac{x(1+4x-4x^2)}{\epsilon}-x(1+4x-4x^2)\ln\left(\frac{\Lambda^2}{m^2}+(1-2x)^2\right)\right]\\ &+\frac{x(1+4x-4x^2)}{[(1-2x)^2]_{++}}+\frac{m^2x(1+4x-4x^2)}{\Lambda^2+m^2(1-2x)^2}-\frac{1}{2}\delta\left(x-\frac{1}{2}\right)\Bigg\}\theta(x)\theta\left(\frac{1}{2}-x\right)+(x\to 1-x).\end{aligned} \tag{B8}$$

Now we have the ultimate result of $\mathcal{I}(x)$:

$$\begin{aligned}\mathcal{I}(x) = \mathcal{I}_1(x)+\mathcal{I}_2(x) = &\frac{C_F g_s^2}{4\pi^2}\Bigg[x\Bigg(\frac{(1+4x-4x^2)}{(1-2x)^2}-\frac{m^2(1+4x-4x^2)}{\Lambda^2+(1-2x)^2m^2}-\frac{\Lambda^2}{\Lambda^2+(1-2x)^2m^2}\\ &+\ln\left(1+\frac{\Lambda^2}{m^2(1-2x)^2}\right)\Bigg)\theta(x)\theta\left(\frac{1}{2}-x\right)+(x\to 1-x)\Bigg]_{++}\\ &+\frac{C_F g_s^2}{4\pi^2}\delta\left(x-\frac{1}{2}\right)\left[\frac{1}{4}\left(\frac{1}{\epsilon}+\ln\mu_{\mathrm{IR}}^2\right)+\mathcal{O}(\epsilon^0)\right],\end{aligned} \tag{B9}$$

which contains the IR pole $\delta(x-\frac{1}{2})/(4\epsilon)$.

We also need to include the effects due to the quark wave function renormalization, as outlined in (25). The Feynman parts of such contributions are

$$\delta Z_q = iC_F g_s^2 \left(\frac{\mu_{\rm IR}^2 e^{\gamma_E}}{4\pi}\right)^\epsilon \int \frac{d^{4-2\epsilon}k}{(2\pi)^{4-2\epsilon}} \bar{u}(p)\gamma^\mu \frac{1}{\not k + \not p - m + i\epsilon}\gamma^+ \times \frac{1}{\not k + \not p - m + i\epsilon}\gamma_\mu u(p)\frac{1}{k^2 + i\epsilon}/[\bar{u}(p)\gamma^+ u(p)], \tag{B10}$$

$$\delta Z_{\bar q} = iC_F g_s^2 \left(\frac{\mu_{\rm IR}^2 e^{\gamma_E}}{4\pi}\right)^\epsilon \int \frac{d^{4-2\epsilon}k}{(2\pi)^{4-2\epsilon}} \bar{v}(p)\gamma^\mu \frac{1}{\not k - \not p - m + i\epsilon}\gamma^+ \times \frac{1}{\not k - \not p - m + i\epsilon}\gamma_\mu v(p)\frac{1}{k^2 + i\epsilon}/[\bar{v}(p)\gamma^+ v(p)]. \tag{B11}$$

These constants are also IR-divergent:

$$(\delta Z_q + \delta Z_{\bar q})\delta\left(x - \frac{1}{2}\right) = -\frac{C_F g_s^2}{4\pi^2}\left[\frac{1}{4}\left(\frac{1}{\epsilon} + \ln\mu_{\rm IR}^2\right) + \mathcal{O}(\epsilon^0)\right]\delta\left(x - \frac{1}{2}\right). \tag{B12}$$

Note the $\delta'(x - \frac{1}{2})$ have canceled between two symmetric pieces under $x \to 1 - x$.

It is reassuring that the IR poles exactly cancel upon summing $\mathcal{I}(x)$ in (B9)) and (B12).

2. Quasi-DA

For the quasi-DA of $J/\psi^\parallel$, we choose n^μ as the spacelike reference vector as specified in (16). The Feynman part of the vertex diagram in (22) is

$$\begin{aligned}
\tilde{\mathcal{I}}(x) &= \frac{C_F}{(2\pi)^{4-2\epsilon}}\left(\frac{\mu_{\rm IR}^2 e^{\gamma_E}}{4\pi}\right)^\epsilon \int d^d k \bar{u}(p)(-ig_s\gamma^\mu)\frac{i}{\not p + \not k - m + i\epsilon}\gamma^z \frac{i}{\not p - \not k - m + i\epsilon} \\
&\quad \times (-ig_s\gamma^\nu)v(p)\frac{-ig_{\mu\nu}}{k^2 + i\epsilon}\delta\left(x - \frac{1}{2} - \frac{k^z}{2p^z}\right)/[\bar{u}(p)\gamma^z v(p)] \\
&= \frac{-ig_s^2 C_F}{(2\pi)^{4-2\epsilon}}\left(\frac{\mu_{\rm IR}^2 e^{\gamma_E}}{4\pi}\right)^\epsilon \frac{2\pi^{1-\epsilon}}{\Gamma(1-\epsilon)}\int_0^\Lambda dk_\perp k_\perp^{1-2\epsilon}\int dk^0 dk^z \\
&\quad \times \frac{(2-2\epsilon)(k^2 - 2k^z(\frac{p^z k^0}{p^0} - k^z)) - 4m^2}{[(p+k)^2 - m^2 + i\epsilon][(p-k)^2 - m^2 + i\epsilon]}\frac{\delta(x - \frac{1}{2} - \frac{k^z}{2p^z})}{k^2 + i\epsilon}.
\end{aligned} \tag{B13}$$

We first perform the k^0 integration by the contour method and then use the δ function to trade the k^z for the dimensionless momentum fraction x. Nevertheless, since the propagators are now quadratic in k^0, the poles are always dispersed in both the upper and lower complex planes, irrespective of the range where x lies. After integrating over k^0 and k^z, we have

$$\begin{aligned}
\tilde{\mathcal{I}}(x) &= \frac{g_s^2 C_F}{(2\pi)^{3-2\epsilon}}\frac{4\pi^{1-\epsilon}\mu_{\rm IR}^{2\epsilon}}{\Gamma(1-\epsilon)}\int_0^\Lambda dk_\perp k_\perp^{1-2\epsilon}\frac{p^z}{4p^0} \\
&\quad \times \left\{\left[\frac{(m^2 + 2(p^z)^2 x)\sqrt{k_\perp^2 + m^2 + 4(p^z)^2 x}(\epsilon - 1) + p^0(4(p^z)^2 x^2(\epsilon - 1) + m^2\epsilon)}{\sqrt{k_\perp^2 + m^2 + 4(p^z)^2 x^2}(m^2 + 2(p^z)^2 x - p^0\sqrt{k_\perp^2 m^2 + 4(p^z)^2 x^2})^2}\right]_{1\,\rm st}\right. \\
&\quad + \left[\frac{-(m^2 + 2(p^z)^2(1-x))\sqrt{k_\perp^2 + m^2 + 4(p^z)^2(1-x)^2}(\epsilon - 1) + p^0(4(p^z)^2(1-x)^2(\epsilon - 1) + m^2\epsilon)}{\sqrt{k_\perp^2 + m^2 + 4(p^z)^2(1-x)^2}(m^2 + 2(p^z)^2(1-x) - p^0\sqrt{k_\perp^2 + m^2 + 4(p^z)^2(1-x)^2})^2}\right. \\
&\quad \left.\left. - \frac{2(m^2 p^0 - (p^z)^2(1-2x)(\sqrt{k_\perp^2 + (p^z)^2(1-2x)^2} - p^0(1-2x))(\epsilon - 1))}{\sqrt{k_\perp^2 + (p^z)^2(1-2x)^2}(p^0\sqrt{k_\perp^2 + (p^z)^2(1-2x)^2} - p^z(1-2x))^2}\right]_{2\,\rm nd}\right\},
\end{aligned} \tag{B14}$$

where $p^0 = \sqrt{(p^z)^2 + m^2}$.

The first piece $\tilde{\mathcal{I}}_1(x)$ (labeled by the subscript 1st) in (B14) is IR finite, because its denominator does not vanish as $k_\perp \to 0$ at $x \to \frac{1}{2}$. After sending $\epsilon \to 0$ and performing the $k_\perp$ integration, we obtain

$$\tilde{\mathcal{I}}_1(x) = \frac{(m^2+4(p^z)^2x(1-x))}{8\pi^2(p^0)^2(1-2x)^2p^z(m^2(p^z)^2(1-2x)^2+\Lambda^2(p^0)^2)} \times [(m^2\Lambda^2\sqrt{m^2+4(p^z)^2x^2}-p^0)+\Lambda^2(p^z)^2(\sqrt{m^2+4(p^z)^2x^2}-2p^0x) + m^2(p^z)^2(1-2x)^2(\sqrt{m^2+4(p^z)^2x^2}-\sqrt{\Lambda^2+m^2+4(p^z)^2x^2})] + \frac{p^z(m^2+2(p^z)^2x)}{16\pi^2(p^0)^3}\left[-\ln\left(\frac{m^2+2(p^z)^2x+p^0\sqrt{\Lambda^2+m^2+4(p^z)^2x^2}}{m^2+2(p^z)^2x-p^0\sqrt{\Lambda^2+m^2+4(p^z)^2x^2}}\right) + \ln\left(\frac{m^2+2(p^z)^2x+p^0\sqrt{m^2+4(p^z)^2x^2}}{m^2+2(p^z)^2x-p^0\sqrt{m^2+4(p^z)^2x^2}}\right)-\ln\left(1+\frac{\Lambda^2(p^0)^2}{m^2(p^z)^2(1-2x)^2}\right)\right]. \tag{B15}$$

The second piece $\tilde{\mathcal{I}}_2(x)$ (denoted with subscript 2nd) in (B14) potentially contains IR singularity at $x=\frac{1}{2}$. Integrating over the transverse momentum by brute force, we obtain

$$\begin{aligned}
\tilde{\mathcal{I}}_2 = \frac{C_F g_s^2 e^{\epsilon\gamma}\mu_{\mathrm{IR}}^{2\epsilon}}{4\pi^2\Lambda^{2\epsilon}}\Bigg[&\frac{\Lambda^2(m^2-2(p^z)^2(x-1))^2\sqrt{m^2+4(p^z)^2(x-1)^2}}{2(p^z)^3m^4(1-2x)^4\Gamma(1-\epsilon)} \\
&\times F_1\left(1-\epsilon,2,-\frac{1}{2},2-\epsilon,-\frac{(p^0)^2\Lambda^2}{m^2(p^z)^2(1-2x)^2},-\frac{\Lambda^2}{m^2+4(p^z)^2(1-x)^2}\right) \\
&-\frac{\Lambda^2(p^z)^2|1-2x|}{m^4(1-2x)^4\Gamma(1-\epsilon)}F_1\left(1-\epsilon,2,-\frac{1}{2},2-\epsilon,-\frac{(p^0)^2\Lambda^2}{m^2(p^z)^2(1-2x)^2},-\frac{\Lambda^2}{(p^z)^2(1-x)^2}\right) \\
&+\frac{p^z\Lambda^{2\epsilon}(p^0)^{2\epsilon-1}}{(1+2\epsilon)\Gamma(1-\epsilon)}\frac{m^2+(p^z)^2(1-2x)^2(\epsilon-1)}{(p^0\sqrt{\Lambda^2+(p^z)^2(1-2x)^2}+(p^z)^2(2x-1))^{1+2\epsilon}} \\
&\times F_1\left(2\epsilon+1;\epsilon,\epsilon;2\epsilon+2;\frac{p^z(p^z(2x-1)+p^0|1-2x|)}{(2x-1)(p^z)^2+p^0\sqrt{\Lambda^2+(p^z)^2(1-2x)^2}},\frac{p^z(p^z(2x-1)-p^0|1-2x|)}{(2x-1)(p^z)^2+p^0\sqrt{\Lambda^2+(p^z)^2(1-2x)^2}}\right) \\
&-\frac{p^z\Lambda^{2\epsilon}(p^0)^{2\epsilon-1}}{2(1+2\epsilon)\Gamma(1-\epsilon)}\frac{m^2\epsilon+4(p^z)^2(1-x)^2(\epsilon-1)}{(p^0\sqrt{\Lambda^2+m^2+4(p^z)^2(1-x)^2}-m^2+2(p^z)^2(x-1))^{1+2\epsilon}} \\
&\times F_1\left(2\epsilon+1,\epsilon,\epsilon,2\epsilon+2,\frac{m^2-2(p^z)^2(x-1)-p^0\sqrt{m^2+4(p^z)^2(x-1)^2}}{m^2-2(p^z)^2(x-1)-p^0\sqrt{\Lambda^2+m^2+4(p^z)^2(x-1)^2}}\right. \\
&\left.\times\frac{m^2-2(p^z)^2(x-1)+p^0\sqrt{m^2+4(p^z)^2(x-1)^2}}{m^2-2(p^z)^2(x-1)-p^0\sqrt{\Lambda^2+m^2+4(p^z)^2(x-1)^2}}\right) \\
&+\frac{\Lambda^2(m^2+2(p^z)^2x)}{4m^2p^zp^0(1-2x)^2\Gamma(1-\epsilon)}\,{}_2F_1\left(1,1-\epsilon;2-\epsilon;-\frac{(p^0)^2\Lambda^2}{m^2(p^z)^2(1-2x)^2}\right) \\
&+\frac{\Lambda^2(m^6-m^4(p^z)^2(x-1)+12m^2(p^z)^4(x-1)^2+2(p^z)^6(4x^3-6x+3))}{2(p^z)^3p^0m^4(1-2x)^4\Gamma(1-\epsilon)} \\
&\times{}_2F_1\left(1,1-\epsilon,2-\epsilon,-\frac{(p^0)^2\mu^2}{m^2(p^z)^2(1-2x)^2}\right)+\frac{p^z\Gamma(2\epsilon+1)}{2(p^0)^{1-2\epsilon}\Gamma(\epsilon+2)} \\
&\times\frac{m^2\epsilon+4(p^z)^2(x-1)^2(\epsilon-1)}{(p^0\sqrt{m^2+4(p^z)^2(1-x)^2}-m^2+2(p^z)^2(x-1))^{1+2\epsilon}} \\
&\times{}_2F_1\left(\epsilon,2\epsilon+1,\epsilon+2,\frac{m^2-2(p^z)^2(x-1)+p^0\sqrt{m^2+4(p^z)^2(x-1)^2}}{m^2-2(p^z)^2(x-1)-p^0\sqrt{m^2+4(p^z)^2(x-1)^2}}\right) \\
&-\frac{p^z\Gamma(2\epsilon+1)}{\Gamma(\epsilon+2)(p^0)^{1-2\epsilon}}(m^2+(p^z)^2(1-2x)^2(\epsilon-1))\left(\frac{1}{p^z(p^0|1-2x|+p^z(2x-1))}\right)^{1+2\epsilon} \\
&\times{}_2F_1\left(\epsilon,2\epsilon+1;\epsilon+2;-\frac{m^2+2(p^z)^2+2p^zp^0\mathrm{sgn}(1-2x)}{m^2}\right)\Bigg],
\end{aligned} \tag{B16}$$

where ${}_2F_1$ is the hypergeometric function, F_1 is the Appell F_1 function, and $\mathrm{sgn}(x)$ denotes the sign function.

In $\tilde{\mathcal{I}}_2(x)$, those terms containing ${}_2F_1$ functions can be manipulated according to the method in Appendix B 1, with the IR pole readily isolated with the aid of distribution identities. Nevertheless, the manipulation of Appell F_1 functions is much more challenging due to its excessive complication. Since the IR singularity is always exactly located at $x=\frac{1}{2}$, we find it beneficial to use the subtraction trick. We first identify the asymptotic behavior of the Appell F_1 function near $x\to\frac{1}{2}$ and then apply the distribution identities to isolate the respective IR poles. The difference between the Appell F_1 and its asymptotic form is IR finite, which is amenable to simple Taylor expansion in powers of ϵ.

The asymptotic forms of Appell F_1 functions required in this work have been tabulated in Appendix D.

Among all terms containing F_1 functions in (B16), only the first one possibly develops an IR singularity. Following the aforementioned technique, we can identify the IR pole associated with this term:

$$\begin{aligned}\tilde{\mathcal{I}}_2^{F_1}(x) &= \frac{C_F g_s^2 e^{\epsilon\gamma}\mu_{\mathrm{IR}}^{2\epsilon}}{4\pi^2\Lambda^{2\epsilon}}\frac{\Lambda^2(m^2-2(p^z)^2(x-1))^2\sqrt{m^2+4(p^z)^2(x-1)^2}}{2(p^z)^3m^4\Gamma(1-\epsilon)(1-2x)^4}\\ &\quad\times F_1\left(1-\epsilon,-\frac{1}{2},1,2-\epsilon,-\frac{(p^0)^2\Lambda^2}{m^2(p^z)^2(1-2x)^2},-\frac{\Lambda^2}{m^2+4(p^z)^2(1-x)^2}\right)\\ &= \frac{C_F g_s^2}{4\pi^2}\left[\frac{3p^z p^0}{16m^2}\left(\frac{1}{\epsilon}+\ln\mu_{\mathrm{IR}}^2\right)+\mathcal{O}(\epsilon^0)\right]\delta\left(x-\frac{1}{2}\right).\end{aligned}\tag{B17}$$

Summing all the IR-divergent terms in (B16), we obtain

$$[\tilde{\mathcal{I}}_2(x)]_{\frac{1}{\epsilon}} = \frac{C_F g_s^2}{4\pi^2}\delta\left(x-\frac{1}{2}\right)\left[\frac{1}{4}\left(\frac{1}{\epsilon}+\ln\mu_{\mathrm{IR}}^2\right)+\mathcal{O}(\epsilon^0)\right],\tag{B18}$$

which has the same single-IR pole as in the light-cone case.

The complete result of $\tilde{\mathcal{I}}$ reads

$$\tilde{\mathcal{I}}(x) = [\tilde{\mathcal{I}}_1(x)|_{\epsilon=0}+\tilde{\mathcal{I}}_2(x)|_{\epsilon=0}]_{++}+\frac{C_F g_s^2}{4\pi^2}\left[\frac{1}{4}\left(\frac{1}{\epsilon}+\ln\mu_{\mathrm{IR}}^2\right)+\mathcal{O}(\epsilon^0)\right]\delta\left(x-\frac{1}{2}\right).\tag{B19}$$

We also need to include the contribution from the quark self-energy diagrams. According to (25), the Feynman part of the quark wave function renormalization constant is

$$\begin{aligned}\delta\tilde{Z}_q &= iC_F g_s^2\left(\frac{\mu_{\mathrm{IR}}^2 e^{\gamma_E}}{4\pi}\right)^{\epsilon}\int\frac{d^{4-2\epsilon}k}{(2\pi)^{4-2\epsilon}}\bar{u}(p)\gamma^\mu\frac{1}{\not k+\not p-m+i\epsilon}\gamma^z\\ &\quad\times\frac{1}{\not k+\not p-m+i\epsilon}\gamma_\mu u(p)\frac{1}{k^2+i\epsilon}/[\bar{u}(p)\gamma^z u(p)],\end{aligned}\tag{B20}$$

$$\begin{aligned}\delta\tilde{Z}_{\bar{q}} &= iC_F g_s^2\left(\frac{\mu_{\mathrm{IR}}^2 e^{\gamma_E}}{4\pi}\right)^{\epsilon}\int\frac{d^{4-2\epsilon}k}{(2\pi)^{4-2\epsilon}}\bar{v}(p)\gamma^\mu\frac{1}{\not k-\not p-m+i\epsilon}\gamma^z\\ &\quad\times\frac{1}{\not k-\not p-m+i\epsilon}\gamma_\mu v(p)\frac{1}{k^2+i\epsilon}/[\bar{v}(p)\gamma^z v(p)].\end{aligned}\tag{B21}$$

Their net contribution is

$$(\delta\tilde{Z}_q+\delta\tilde{Z}_{\bar{q}})\delta\left(x-\frac{1}{2}\right) = -\frac{C_F g_s^2}{4\pi^2}\left[\frac{1}{4}\left(\frac{1}{\epsilon}+\ln\mu_{\mathrm{IR}}^2\right)+\mathcal{O}(\epsilon^0)\right]\delta\left(x-\frac{1}{2}\right).\tag{B22}$$

It is straightforward to check that the single IR pole cancels between (B19) and (B22).

APPENDIX C: DISTRIBUTION IDENTITIES

In DR, the IR divergences usually originate from terms such as $|1/2-x|^{-1-2\epsilon}$, $|1/2-x|^{-1-2\epsilon}\ln|1/2-x|$, and $|1/2-x|^{-2-2\epsilon}$, etc. In this work, the following distribution identities have been utilized to express the above singular structures as the IR pole together with distribution functions:

$$\lim_{\epsilon\to 0}\int_0^{\frac{1}{2}} dx g(x)\times\left|\frac{1}{2}-x\right|^{-1-2\epsilon} = \int_0^{\frac{1}{2}} dx g(x)\times\left\{\left(-\frac{1}{2\epsilon}-\ln 2\right)\delta\left(x-\frac{1}{2}\right)\right\}+\left[\frac{1}{\frac{1}{2}-x}\right]_+\Bigg\}, \quad \text{(C1a)}$$

$$\lim_{\epsilon\to 0}\int_{\frac{1}{2}}^{1} dx g(x)\times\left|\frac{1}{2}-x\right|^{-1-2\epsilon} = \int_{\frac{1}{2}}^{1} dx g(x)\times\left\{\left(-\frac{1}{2\epsilon}-\ln 2\right)\delta\left(x-\frac{1}{2}\right)+\left[\frac{1}{x-\frac{1}{2}}\right]_+\right\}, \quad \text{(C1b)}$$

$$\lim_{\epsilon\to 0}\int_0^{\frac{1}{2}} dx g(x)\times\left|\frac{1}{2}-x\right|^{-1-2\epsilon}\ln\left|\frac{1}{2}-x\right| = \int_0^{\frac{1}{2}} dx g(x)\times\left\{\left[-\frac{1}{4\epsilon^2}+\frac{\ln^2 2}{2}\right]\delta\left(x-\frac{1}{2}\right)+\left[\frac{\ln\left(\frac{1}{2}-x\right)}{\frac{1}{2}-x}\right]_+\right\}, \quad \text{(C2a)}$$

$$\lim_{\epsilon\to 0}\int_{\frac{1}{2}}^{1} dx g(x)\times\left|\frac{1}{2}-x\right|^{-1-2\epsilon}\ln\left|\frac{1}{2}-x\right| = \int_{\frac{1}{2}}^{1} dx g(x)\times\left\{\left[-\frac{1}{4\epsilon^2}+\frac{\ln^2 2}{2}\right]\delta\left(x-\frac{1}{2}\right)+\left[\frac{\ln\left(x-\frac{1}{2}\right)}{x-\frac{1}{2}}\right]_+\right\}, \quad \text{(C2b)}$$

$$\lim_{\epsilon\to 0}\int_0^{\frac{1}{2}} dx g(x)\times\left|\frac{1}{2}-x\right|^{-2-2\epsilon} = \int_0^{\frac{1}{2}} dx g(x)\times\left\{\left(-\frac{1}{2\epsilon}-\ln 2\right)\delta'\left(x-\frac{1}{2}\right)-2\delta\left(x-\frac{1}{2}\right)+\left[\frac{1}{(\frac{1}{2}-x)^2}\right]_{++}\right\}, \quad \text{(C3a)}$$

$$\lim_{\epsilon\to 0}\int_{\frac{1}{2}}^{1} dx g(x)\times\left|\frac{1}{2}-x\right|^{-2-2\epsilon} = \int_{\frac{1}{2}}^{1} dx g(x)\times\left\{\left(\frac{1}{2\epsilon}+\ln 2\right)\delta'\left(x-\frac{1}{2}\right)-2\delta\left(x-\frac{1}{2}\right)+\left[\frac{1}{(\frac{1}{2}-x)^2}\right]_{++}\right\}. \quad \text{(C3b)}$$

The IR divergence is represented by ϵ^{-n}. The above distribution identities should be understood to be convolved with a test function $g(x)$ that is regular at $x=\frac{1}{2}$. The double pole ϵ^{-2} in (C2) stems from the coupled soft and light-cone (axial) singularity.

APPENDIX D: ASYMPTOTIC FORM OF APPELL F_1 FUNCTIONS AND POLE STRUCTURES

When computing the one-loop corrections to the quasi-DAs, we have encountered numerous Appell F_1 functions. Here we present the asymptotic form of the encountered Appell F_1 functions near $x=\frac{1}{2}$:

$$F_1\left(1-\epsilon,-\frac{1}{2},1,2-\epsilon,-\frac{(p^0)^2\Lambda^2}{m^2(p^z)^2(1-2x)^2},-\frac{\Lambda^2}{m^2+4(p^z)^2(1-x)^2}\right)$$
$$\to(1-2x)^4\left[\frac{\Gamma(2-\epsilon)\Gamma(1+\epsilon)}{\Gamma(1-\epsilon)}\left(\frac{p^0\Lambda}{p^z m}\right)^{2\epsilon-2}|1-2x|^{-2-2\epsilon}-\frac{1-\epsilon}{(1+\epsilon)\Gamma(1-\epsilon)}\left(\frac{p^z m}{p^0\Lambda}\right)^4\right], \quad \text{(D1a)}$$

$$F_1\left(1-\epsilon,-\frac{1}{2},1,2-\epsilon,-\frac{\Lambda^2}{(p^z)^2(1-2x)^2},-\frac{(p^0)^2\Lambda^2}{m^2(p^z)^2(1-2x)^2}\right)$$
$$\to(1-2x)^3\left[\frac{m^2\Lambda}{(p^0)^2p^z}\frac{2(p^z)^2(1-\epsilon)}{(1-2\epsilon)\mu^2}(1-2x)^{-2}+\frac{\Gamma(2-\epsilon)\Gamma(\epsilon-\frac{1}{2})}{\sqrt{\pi}}\left(\frac{p^z}{\Lambda}\right)^{3-2\epsilon}\right.$$
$$\left.\times{}_2F_1\left(1,-\frac{1}{2}+\epsilon,\frac{1}{2},\left(\frac{p^z}{p^0}\right)^2\right)|1-2x|^{-1-2\epsilon}\right], \quad \text{(D1b)}$$

$$F_1\left(1-\epsilon,-\frac{1}{2},1,2-\epsilon,-\frac{\Lambda^2}{m^2+4(p^z)^2x^2},-\frac{(p^0)^2\Lambda^2}{m^2(p^z)^2(1-2x)^2}\right)$$
$$\to(1-2x)^3\left[\frac{m^2(p^z)^2}{(p^0)^2\Lambda^2}\left(-\frac{1-\epsilon}{\epsilon}\,{}_2F_1\left(-\frac{1}{2},-\epsilon,1-\epsilon,-\frac{\Lambda^2}{(p^0)^2}\right)+\frac{(p^z\Lambda)^2}{(p^0)^4}\,{}_2F_1\left(\frac{1}{2},1-\epsilon,2-\epsilon-\frac{\Lambda^2}{(p^0)^2}\right)\right)|1-2x|^{-1}\right.$$
$$\left.+\left(\frac{mp^z}{\Lambda p^0}\right)^{2-2\epsilon}|1-2x|^{-1-2\epsilon}\Gamma(2-\epsilon)\Gamma(\epsilon)\right]. \tag{D1c}$$

Although these Appell F_1 functions vanish at $x=\frac{1}{2}$, they are usually accompanied with $(1-2x)^{-n}$ ($n=3$, 4). The subtraction algorithm can be applied to isolate their divergent pieces from finite ones.

We take (B17) as an example:

$$\begin{aligned}\tilde{\mathcal{I}}_2^{F_1}(x)&=\frac{C_F g_s^2 e^{\epsilon\gamma_E}\mu_{\rm IR}^{2\epsilon}}{4\pi^2\Lambda^{2\epsilon}}\frac{\Lambda^2(m^2-2(p^z)^2(x-1))^2\sqrt{m^2+4(p^z)^2(x-1)^2}}{2(p^z)^3m^4\Gamma(1-\epsilon)(1-2x)^4}\\&\quad\times F_1\left(1-\epsilon,-\frac{1}{2},1,2-\epsilon,-\frac{(p^0)^2\Lambda^2}{m^2(p^z)^2(1-2x)^2},-\frac{\Lambda^2}{m^2+4(p^z)^2(1-x)^2}\right)\\&=\tilde{\mathcal{I}}_2^{F_1}(x)|_{\rm asym}+\{\tilde{\mathcal{I}}_2^{F_1}(x)-[\tilde{\mathcal{I}}_2^{F_1}(x)]_{\rm asym}\}|_{\epsilon=0}+\mathcal{O}(\epsilon^1),\end{aligned} \tag{D2}$$

where the first term denotes the asymptotic form of $\tilde{\mathcal{I}}_2^{F_1}(x)$ and the second term denotes the subtracted part. The subtracted part is regular at $x=\frac{1}{2}$; thereby, one can simply set $\epsilon\to 0$ in it.

The asymptotic part reads

$$\begin{aligned}\tilde{\mathcal{I}}_2^{F_1}(x)|_{\rm asym}&=\frac{C_F g_s^2 e^{\epsilon\gamma}\mu_{\rm IR}^{2\epsilon}}{4\pi^2\Lambda^{2\epsilon}}\frac{\Lambda^2(m^2-2(p^z)^2(x-1))^2\sqrt{m^2+4(p^z)^2(x-1)^2}}{2(p^z)^3m^4\Gamma(1-\epsilon)}\\&\quad\times\left(\frac{\Gamma(2-\epsilon)\Gamma(1+\epsilon)}{\Gamma(1-\epsilon)}\left(\frac{p^0\Lambda}{p^zm}\right)^{2\epsilon-2}(1-2x)^{-2-2\epsilon}-\frac{1-\epsilon}{(1+\epsilon)\Gamma(1-\epsilon)}\left(\frac{p^zm}{p^0\Lambda}\right)^4\right).\end{aligned} \tag{D3}$$

Rewriting $(1-2x)^{2+2\epsilon}$ through the distribution identity in (C3b) leads to

$$\begin{aligned}\tilde{\mathcal{I}}_2^{F_1}(x)|_{\rm asym}&=\frac{C_F g_s^2 e^{\epsilon\gamma}\mu_{\rm IR}^{2\epsilon}}{4\pi^2\Lambda^{2\epsilon}}\frac{\Lambda^2(m^2-2(p^z)^2(x-1))^2\sqrt{m^2+4(p^z)^2(x-1)^2}}{2(p^z)^3m^4\Gamma(1-\epsilon)}\\&\quad\times\left(\frac{\Gamma(2-\epsilon)\Gamma(1+\epsilon)}{\Gamma(1-\epsilon)}\left(\frac{p^0\Lambda}{mp^z}\right)^{2\epsilon-2}\frac{1}{2^{2+2\epsilon}}\left(\left(-\frac{1}{2\epsilon}-\log 2\right)\delta'\left(x-\frac{1}{2}\right)\right.\right.\\&\quad\left.\left.-2\delta\left(x-\frac{1}{2}\right)+\left[\frac{1}{(\frac{1}{2}-x)^2}\right]_{++}\right)-\frac{1-\epsilon}{(1+\epsilon)\Gamma(1-\epsilon)}\frac{m^4(p^z)^4}{(p^0)^4\Lambda^4}\right).\end{aligned} \tag{D4}$$

Therefore, the IR pole of $\tilde{\mathcal{I}}_2^{F_1}$ becomes

$$(\tilde{\mathcal{I}}_2^{F_1})_{\frac{1}{\epsilon}}=\frac{C_F g_s^2}{4\pi^2}\left(\frac{3p^zp^0}{16m^2}\right)\left(\frac{1}{\epsilon}+\ln\mu_{\rm IR}^2\right)\delta\left(x-\frac{1}{2}\right). \tag{D5}$$

[1] J. C. Collins, D. E. Soper, and G. F. Sterman, Adv. Ser. Dir. High Energy Phys. **5**, 1 (1989).
[2] J. C. Collins and D. E. Soper, Nucl. Phys. **B194**, 445 (1982).
[3] C. Alexandrou, M. Constantinou, S. Dinter, V. Drach, K. Hadjiyiannakou, K. Jansen, G. Koutsou, and A. Vaquero, J. High Energy Phys. 06 (2015) 068.
[4] P. Hagler *et al.* (LHPC Collaboration), Phys. Rev. D **77**, 094502 (2008).
[5] B. U. Musch, P. Hagler, M. Engelhardt, J. W. Negele, and A. Schafer, Phys. Rev. D **85**, 094510 (2012).
[6] V. M. Braun, S. Collins, M. Göckeler, P. Pérez-Rubio, A. Schäfer, R. W. Schiel, and A. Sternbeck, *Proc. Sci.*, QCDEV2015 (2015) 009 [arXiv:1510.07429].
[7] J. Gao, M. Guzzi, J. Huston, H.-L. Lai, Z. Li, P. Nadolsky, J. Pumplin, D. Stump, and C.-P. Yuan, Phys. Rev. D **89**, 033009 (2014).
[8] A. D. Martin, W. J. Stirling, R. S. Thorne, and G. Watt, Eur. Phys. J. C **63**, 189 (2009).
[9] R. D. Ball *et al.* (NNPDF Collaboration), J. High Energy Phys. 04 (2015) 040.
[10] X. Ji, Phys. Rev. Lett. **110**, 262002 (2013).
[11] X. Ji, Sci. China Phys. Mech. Astron. **57**, 1407 (2014).
[12] X. Ji, J. H. Zhang, and Y. Zhao, Phys. Rev. Lett. **111**, 112002 (2013).
[13] X. Ji, J. H. Zhang, and Y. Zhao, Phys. Lett. B **743**, 180 (2015).
[14] X. Xiong, X. Ji, J. H. Zhang, and Y. Zhao, Phys. Rev. D **90**, 014051 (2014).
[15] Y.-Q. Ma and J.-W. Qiu, arXiv:1404.6860.
[16] X. Ji, A. Schäfer, X. Xiong, and J. H. Zhang, Phys. Rev. D **92**, 014039 (2015).
[17] X. Ji, P. Sun, X. Xiong, and F. Yuan, Phys. Rev. D **91**, 074009 (2015).
[18] X. Ji and J. H. Zhang, Phys. Rev. D **92**, 034006 (2015).
[19] H.-W. Lin, J.-W. Chen, S. D. Cohen, and X. Ji, Phys. Rev. D **91**, 054510 (2015).
[20] C. Alexandrou, K. Cichy, V. Drach, E. Garcia-Ramos, K. Hadjiyiannakou, K. Jansen, F. Steffens, and C. Wiese, Phys. Rev. D **92**, 014502 (2015).
[21] J. W. Chen, S. D. Cohen, X. Ji, H. W. Lin and J. H. Zhang, Nucl. Phys. **B911**, 246 (2016).
[22] C. Alexandrou, K. Cichy, M. Constantinou, K. Hadjiyiannakou, K. Jansen, F. Steffens, and C.~Wiese, arXiv:1610.03689.
[23] T. Ishikawa, Y. Q. Ma, J. W. Qiu and S. Yoshida, arXiv:1609.02018.
[24] J. W. Chen, X. Ji, and J. H. Zhang, arXiv:1609.08102.
[25] L. Gamberg, Z. B. Kang, I. Vitev, and H. Xing, Phys. Lett. B **743**, 112 (2015).
[26] G. T. Bodwin, E. Braaten, and G. P. Lepage, Phys. Rev. D **51**, 1125 (1995); **55**, 5853 (1997).
[27] J. P. Ma and Z. G. Si, Phys. Lett. B **647**, 419 (2007).
[28] G. Bell and T. Feldmann, J. High Energy Phys. 04 (2008) 061.
[29] X. P. Wang and D. Yang, J. High Energy Phys. 06 (2014) 121.
[30] K. A. Olive *et al.* (Particle Data Group Collaboration), Chin. Phys. C **38**, 090001 (2014).
[31] E. Braaten, K. m. Cheung, and T. C. Yuan, Phys. Rev. D **48**, 4230 (1993).
[32] E. Braaten and T. C. Yuan, Phys. Rev. Lett. **71**, 1673 (1993).
[33] Y. Jia and D. Yang, Nucl. Phys. **B814**, 217 (2009).
[34] Y. Jia, J. X. Wang, and D. Yang, J. High Energy Phys. 10 (2011) 105.
[35] M. Beneke and V. A. Smirnov, Nucl. Phys. **B522**, 321 (1998).
[36] E. Braaten and Y. Q. Chen, Phys. Rev. D **54**, 3216 (1996).
[37] V. V. Braguta, A. K. Likhoded, and A. V. Luchinsky, Phys. Lett. B **646**, 80 (2007).
[38] M. Beneke, A. Signer, and V. A. Smirnov, Phys. Rev. Lett. **80**, 2535 (1998).
[39] A. Czarnecki and K. Melnikov, Phys. Rev. Lett. **80**, 2531 (1998).
[40] A. Czarnecki and K. Melnikov, Phys. Lett. B **519**, 212 (2001).
[41] G. P. Lepage and S. J. Brodsky, Phys. Lett. B **87**, 359 (1979).
[42] A. V. Efremov and A. V. Radyushkin, Phys. Lett. B **94**, 245 (1980).
[43] Y. Q. Ma, J. W. Qiu, and H. Zhang, Phys. Rev. D **89**, 094029 (2014).
[44] G. P. Lepage and S. J. Brodsky, Phys. Rev. D **22**, 2157 (1980).